Developmental Biology **230,** 278–301 (2001)
doi:10.1006/dbio.2000.9995, available online at http://www.idealibrary.com on IDEAL®

metadata, citation and similar papers at core.ac.uk
brought to you by CORE
provided by Elsevier - Publisher Connector

An Atlas of Embryonic and Early Larval Development

Sumio Isogai,*,† Masaharu Horiguchi,† and Brant M. Weinstein*,[1]

**Laboratory of Molecular Genetics, NICHD, NIH, Building 6B, Room 309, 6 Center Drive, Bethesda, Maryland 20892; and †Department of Anatomy, School of Medicine, Iwate Medical University, Morioka 020–8505, Japan*

We have used confocal microangiography to examine and describe the vascular anatomy of the developing zebrafish, *Danio rerio*. This method and the profound optical clarity of zebrafish embryos make it possible to view the entire developing vasculature with unprecedented resolution. A staged series of three-dimensional images of the vascular system were collected beginning shortly after the onset of circulation at 1 day postfertilization through early- to midlarval stages at approximately 7 days postfertilization. Blood vessels in every region of the animal were imaged at each stage, and detailed "wiring patterns" were derived describing the interconnections between every major vessel. We present an overview of these data here in this paper and in an accompanying Web site "The interactive atlas of zebrafish vascular anatomy" online at (http://eclipse.nichd.nih.gov/nichd/lmg/redirect.html). We find a highly dynamic but also highly stereotypic pattern of vascular connections, with different sets of primitive embryonic vessels severing connections and rewiring in new configurations according to a reproducible plan. We also find that despite variation in the details of the vascular anatomy, the basic vascular plan of the developing zebrafish shows strong similarity to that of other vertebrates. This atlas will provide an invaluable foundation for future genetic and experimental studies of vascular development in the zebrafish.

Key Words: **zebrafish; vascular anatomy; blood vessels; fluorescent dye confocal microangiography; confocal microscopy.**

INTRODUCTION

The development of the vasculature has been extensively examined in a variety of vertebrates, but has traditionally been difficult to study *in vivo* using experimental embryologic or classical genetic methods. Blood vessels are one of the few major organ systems with no reasonably direct homologue in nonvertebrate species, precluding analysis in genetically accessible nonvertebrates. In *Drosophila*, for example, a primitive heart and blood (hemolymph) are present but hemolymph circulates through spaces that do not possess a cellular endothelial lining. In vertebrates, a functional vasculature is essential for embryonic survival, and it is often difficult to observe blood vessels directly in living embryos due to their opacity or development internal to the mother. Teleost fish, and the zebrafish in particular, provide a number of advantages in this regard. The small size and fecundity of zebrafish, and the development external to its mother and optical clarity of the zebrafish embryo, provide great advantages for experimental and genetic analysis of vascular development. Because of their small size, zebrafish embryos also receive enough oxygen by passive diffusion to survive and continue to develop in reasonably normal fashion for several days even in the complete absence of blood circulation, facilitating phenotypic analysis of animals with circulatory defects. This combination of features has made it possible to perform large-scale forward-genetic screens to isolate embryonic and early larval lethal mutations in the zebrafish (Driever *et al*., 1996; Haffter *et al*., 1996), including many that specifically affect the circulatory system (Stainier *et al*., 1995; Weinstein *et al*., 1995). The optical clarity and accessibility of the zebrafish embryo also permit efficient application of experimental embryologic methods for *in vivo* analysis of vascular development, notably confocal microangiography (Weinstein *et al*., 1995).

In order to fully exploit the advantages of the zebrafish for studying vascular development, however, there must be sufficient knowledge of the normal pattern of the vascula-

[1] To whom correspondence should be addressed.

0012-1606/01 $35.00

ture in this species to enable detection of mutants, interpretation of the results of experimental or genetic perturbations, and cross-species comparisons. All of these are dependent on having a detailed, accurate, staged description of the normal vascular anatomy. The only previously published description of the vascular anatomy of the developing zebrafish is a 1973 study by Jean-Pierre Rieb (Rieb, 1973). Using direct visual observation and camera lucida drawings, he described vascular patterns in developing embryos up to 33 h postfertilization. The methods employed and restricted temporal scope of this study have limited its usefulness, however. Studies of the developing vasculature have been performed in other teleosts, and these have suggested that despite many specific vascular adaptations to different anatomical and environmental requirements, there is a great deal of conservation between the basic layout of the circulatory system in fish and other vertebrates. Swaen and Brachet's study (Swaen and Brachet, 1899) provided the first detailed report in the scientific literature of the emergence of the teleost vasculature, describing the formation of the primitive erythrocytes and first axial vessels of the trunk. Subsequent studies (most frequently using Salmonids) provided more in-depth description of the formation of different portions of the early teleost vascular system (Disler, 1957; Grodzinski, 1925; Grodzinski and Hoyer, 1938; Kilarski, 1958; Olko, 1955; Strawinski, 1949; Vernier, 1969). Many early teloest researchers believed that blood vessels formed in a different manner in fish than in other vertebrates, noting in particular the intraembryonic origin of vessel progenitors. Vessels in birds and mammals were historically thought to arise by growth into the embryo from extraembryonic tissues, a view refuted by many experimental studies (for example, Reagan, 1915; Sabin, 1917). Ura and colleagues published many detailed comparative studies on the development of the vascular system in a wide variety of species, including *Amphiouxus* (Ura, 1949), *Lampetra* (Yamada, 1951), *Trygon* (Ura, 1956), *Neoceratodus* (Saito, 1984), *Hynobius* (Aoyama, 1956), *Caretta* (Kawanishi, 1956), *Gallus* (Isida, 1956), *and Cricetus* (Tada, 1956), noting both similarities and some differences in the development of the embryonic vasculature of teleosts (see Discussion). More recent studies (e.g., Colle-Vandevelde, 1963; Isogai and Horiguchi, 1997; Iuchi and Yamamoto, 1983) have resolved at least some of the apparent differences and further supported the view that the earliest blood and blood vessels of developing teleosts are similar to those of other vertebrates in most respects.

Here, we present a detailed and complete study of the vascular anatomy of the developing zebrafish embryo and early larva, prepared using confocal microangiography (Weinstein *et al*., 1995). This technique relies on the small size and high degree of optical clarity of the developing zebrafish, features that make it possible to image vessels throughout the entire depth of the animal. Unlike "traditional" methods used to delineate the vasculature such as injection of India ink, colored dyes, or plastic resins, confocal microangiography does not kill or even significantly harm the specimens, and images are collected from living animals with an active, fully inflated circulation. The small fluorescent microspheres employed penetrate even the smallest patent spaces, and the resolution of the method is limited only by the optical resolution of the microscope used. Vessels that would be obscured by other, surrounding vessels when previous methods were used are readily imaged using confocal microangiography. Furthermore, the data can be directly and immediately rendered into three-dimensional images. Using confocal microangiography, we have imaged, examined, and described vessels in every region of the zebrafish embryo and early larva, and at all developmental stages from the initiation of circulation at 1 day postfertilization through early larvae at 7 days postfertilization. These data are described in detail here and online at "The interactive atlas of zebrafish vascular anatomy" (http://eclipse.nichd.nih.gov/nichd/lmg/redirect.html).

MATERIALS AND METHODS

Zebrafish Methods

Zebrafish (*Danio rerio*) embryos were obtained from natural spawnings of wild-type or *albino* mutant laboratory lines. Embryos were raised and fish were maintained as described (Westerfield, 1995). Embryos were incubated at 28.5°C in 30% Danieu's solution (Westerfield, 1995) and staged as described (Kimmel *et al*., 1995; Westerfield, 1995). Some wild-type embryos used at 1.5 days or later were treated with 1-phenyl-2-thiourea (PTU; Sigma) in 30% Danieu's solution to inhibit pigment formation (Westerfield, 1995), using the following regimen. Embryos were soaked in 0.003% PTU/30% Danieu's solution for 2 h on the mornings of days 1, 2, and 3 postfertilization but otherwise maintained in 30% Danieu's solution without PTU. This treatment regimen did not appear to have a significant effect on vascular development. Untreated wild-type or albino mutant 1 to 7-day-old embryos had microangiographic patterns indistinguishable from those of similarly staged PTU-treated embryos.

Confocal Microangiography

Microangiography of zebrafish embryos and larvae was performed essentially as described previously (Weinstein *et al*., 1995). A detailed protocol for this procedure is provided online at our interactive Web site (http://eclipse.nichd.nih.gov/nichd/lmg/redirect.html) The reconstructions shown in all of the figures in this paper are single-view "2-D" reconstructions of collected image Z-series stacks, reconstructed at a single angle of zero degrees. Three-dimensional reconstructions of these same images, and others, are available for viewing online at the Web site.

Berlin-Blue Dye Injection

We prepared a complete series of dye-injected specimens at various stages from 1-day through 7-day embryos in order to permit independent confirmation of vascular wiring patterns visualized by confocal microangiography and to allow description of a few areas that were difficult to image using the latter method. For dye injection, an anesthetized living embryo was first embedded in

Copyright © 2001 by Academic Press. All rights of reproduction in any form reserved.

low-melt agarose in order to hold it in place. After embedding, the sinus venosus was incised to allow blood drainage, and then Berlin-blue solution (0.75%) was injected via glass capillaries inserted into either the dorsal aorta or the caudal artery. After perfusion the embryos were fixed in neutral 10% formalin. The specimens were viewed, photographed, and as necessary dissected using a stereomicroscope. Wiring diagrams were traced over photographic images using Adobe Photoshop, as described below.

Wiring Diagrams

Drawings detailing vascular wiring patterns were prepared using Adobe Photoshop. Black/gray drawings were traced over the single-view (zero-degree angle) reconstructions of confocal angiograms prepared using Metamorph (Universal Imaging). For the most part, vessels in black are arterial and vessels in gray are venous. Transitions between these vessels are shaded as such. When vessels leave the region imaged in the confocal angiogram, they are shown fading out into white. For complex, multilayered wiring diagrams (dorsal views of cranial vessels at later stages of development) confocal image stacks were subdivided into a set of four or five partially overlapping smaller stacks, each of which was separately reconstructed into a single-view (zero-degree angle) image. Black/gray drawings were traced separately over each of the "subreconstructions" of the image stack. Parsing wiring patterns frequently required 3-D visualization of the data via reconstructed image rotation movies, red–green stereo pairs, or most often examination of the raw data stack (see our Web site at (http://eclipse.nichd.nih.gov/nichd/lmg/redirect.html) to access these 3-D images). The patterns shown in our drawings may not always be obvious from the corresponding angiography image shown in the figures in this paper, but are nevertheless to the best of our ability true and correct representations of the actual three-dimensional configurations of the vessels.

Vessel Nomenclature

Prior to our undertaking this work, there were no comprehensive standard references for comparing the vascular anatomy of developing teleost fish to that of other vertebrates. Previous detailed descriptive studies of teleost vascular development were performed almost exclusively using salmonids (zebrafish are cyprinids) and were generally limited to particular subportions of the vasculature and/or particular embryonic stages (see Introduction). We also examined a large number of previous reports on the general embryonic development of other teleosts (most not cited in this study). However, the fragmentary description of the vascular anatomy in most of these reports, and the fact that names for vessels were often adopted without sufficient consideration having been given to their comparative anatomy, limited their usefulness. In order to conform as much as possible to the nomenclature accepted for vertebrates in general, we have therefore relied extensively on standard, landmark references for the vascular anatomy of other developing vertebrates. A listing of these is provided online at our Web site (http://eclipse.nichd.nih.gov/nichd/lmg/redirect.html). To the extent that there are limitations to our ability to make definitive assignments of vessel nomenclature, our names may be reconsidered if future studies warrant this (see "Nomenclature" at the Web site). Table 1 lists the designated names and abbreviations of all vessels named in the diagrams and text of this paper.

RESULTS

1–1.2 Days Postfertilization

Circulation begins in the zebrafish embryo at approximately 24–26 h postfertilization (hpf). Initially blood flows through a simple single circulatory loop (Fig. 1A). Blood exits the heart through the bulbus arteriosus and the ventral aorta then branches to the right and left into the mandibular (first) aortic arches. The arches empty directly into the right- and left-lateral dorsal aortas (LDA), which run caudally, approaching one another and then merging in the cranial trunk to form a single medial dorsal aorta (DA). The single dorsal aorta continues into the tail [the portion caudal to the anal pore is designated the caudal artery (CA)] and then turns 180° at its caudal-most end to empty into the caudal vein (CV). At or after this stage, the CV becomes a sinus or a braided plexus of vessels rather than a single distinct channel like the dorsal aorta or caudal artery. The CV remains in this form for many days hence. Circulation from this caudal venous plexus continues into the trunk, becoming a single distinct posterior cardinal vein (PCV) cranial to the anal pore. The cardinal vein splits into a pair of vessels in the cranial trunk, just caudal to the radix of the aorta. The posterior cardinals each empty into a large sinus, the duct of Cuvier (DC) or future common cardinal vein (CCV), which fans out across the yolk cell on either side, coming together cranioventrally at the sinus venosus of the heart. There are no vitelline arteriolae (transverse vessels) per se in the zebrafish; the DC presumably fulfills this function. It should be noted that, unlike in many other vertebrates, in zebrafish embryos the DA and PCV are single medial unpaired tubes at the time circulation begins in the trunk, rather than a pair of more lateral vessels. Amphibians and reptiles also have a medial DA; although similar to mammals and avians, their PCV is present as paired lateral vessels throughout the trunk.

Shortly after the commencement of this initial circulatory loop, a second, rostral loop comes on line (Fig. 1B). Blood exiting the first aortic arches now flows bidirectionally, caudally into the lateral dorsal aortae and rostrally into the primitive internal carotid arteries (PICA; Figs. 1C and 1D). Each PICA initially divides into two branches. The caudal division of the internal carotid artery (CaDI) dives deep inside the embryo, looping dorsally and caudally to join the equivalent branch from the other side via the basal communicating artery (BCA) at the brain midline (Figs. 1B, 2G, and 14A). The cranial division of internal carotid artery (CrDI) goes rostral to the optic capsule, then curves caudally, emptying into the primordial midbrain channel (PMBC) (Figs. 1C–1F). The PMBC continues caudally to the primordial hindbrain channel (PHBC). The anterior cerebral vein (ACeV) also branches from it at 1.3 dpf.

The midcerebral veins (MCeV) take off from the PHBC–PMBC junction and extend bilaterally up along the midbrain–hindbrain boundary toward the dorsal midline of the head (Figs. 1C–1F). At this stage these vessels do not yet meet at the

Copyright © 2001 by Academic Press. All rights of reproduction in any form reserved.

TABLE 1

Glossary of Vascular Nomenclature: Abbreviations Used in the Diagrams in This Paper and the Corresponding Names of the Designated Vessels

AA1	Mandibular arch	MMCtA	Middle mesencephalic central artery
AA2	Hyoid arch	MPLV	Median palatocerebral vein
AA3	First branchial arch	MsA	Mesencephalic artery
AA4	Second branchial arch	MsV	Mesencephalic vein
AA5	Third branchial arch	MtA	Metencephalic artery
AA6	Fourth branchial arch	NA	Nasal artery
ABA	Afferent branchial artery	NCA	Nasal ciliary artery
ABE	Efferent branchial artery	NV	Nasal vein
ACeV	Anterior (rostral) cerebral vein	OA	Optic artery
ACV	Anterior (rostral) cardinal vein	OpV	Ophthalmic vein
ALB	Laminar branchial artery	ORA	Opercular artery
ALBA	Afferent laminar branchial artery	OV	Optic vein
ALBE	Efferent laminar branchial artery	P	Pronephric glomus
AMA	Anterior (rostral) mesenteric artery	PA	Pectoral artery
AMCtA	Anterior (rostral) mesencephalic central artery	PAV	Parachordal vessel
BA	Basilar artery	PBA	Pseudobranchial artery
BCA	Basal communicating artery	PCeV	Posterior (caudal) cerebral vein
BuA	Bulbus arteriosus	PCS	Posterior (caudal) communicating segment
CA	Caudal artery	PCV	Posterior (caudal) cardinal vein
CaDI	Caudal division of the internal carotid artery	PHBC	Primordial hindbrain channel
CCtA	Cerebellar central artery	PHS	Primary head sinus
CCV	Common cardinal vein (= duct of Cuvier or DC)	PICA	Primitive internal carotid artery
CMV	Communicating vessel	PLA	Palatocerebral artery
CrDI	Cranial division of the internal carotid artery	PLAJ	Junction of the palatocerebral arteries
CtA	Central artery	PLV	Palatocerebral vein
CV	Caudal vein	PMA	Posterior (caudal) mesenteric artery
CVP	Choroidal vascular plexus	PMBC	Primordial midbrain channel
DA	Dorsal aorta	PMCtA	Posterior (caudal) mesencephalic central artery
DC	Duct of Cuvier (= common cardinal vein or CCV)	PMsA	Primitive mesencephalic artery
DCV	Dorsal ciliary vein	PPrA	Primitive prosencephalic artery
DLAV	Dorsal longitudinal anastomotic vessel	PrA	Prosencephalic artery
DLV	Dorsal longitudinal vein	PV	Pectoral vein
DMJ	Dorsal midline junction	SBA	Swim bladder artery
H	Heart	Se	Intersegmental vessel
HA	Hypobranchial artery	SeA	Intersegmental artery
HPV	Hepatic portal vein	SeV	Intersegmental vein
ICA	Internal carotid artery	SIA	Supraintestinal artery
IOC	Inner optic circle	SIV	Subintestinal vein
L	Liver	SV	Sinus venosus
LB	Lateral branch	VA	Ventral aorta
LDA	Lateral dorsal aorta	VI	Ventral intersegmental/intercostal
MCeV	Middle cerebral vein	VTA	Vertebral artery

midline and have no arterial feed. The PHBC are located medial to the cranial nerves and the otic capsule, running caudally from the base of the MCeV to the base of the future posterior cerebral veins (PCeV). At the base of the future PCeVs blood then flows ventrolaterally from the PHBC, via short segments near the caudal end of the otic capsule, down to the anterior cardinal veins (ACV). The ACV joins with the PCV at approximately the same rostral–caudal level as the radix of the aorta to form the CCV/DC. The more rostral portion of the ACV (primary head sinus, PHS) located ventrolaterally to the otic capsule, has not yet formed.

1.5 Days Postfertilization

By 1.5 dpf, many developing intersegmental arteries and veins (SeA, SeV) can be seen in the trunk (Fig. 2A). At slightly earlier stages intersegmental vessels (Se) can be seen sprouting and elongating dorsally up from the DA and PCV below (Fig. 2H). The sprouts form a "T" in the most dorsal regions of the trunk and their tips anastamose longitudinally to form a right and left pair of dorsal longitudinal anastamotic vessels (DLAVs). There are few or no interconnections between the DLAVs at earlier stages.

Copyright © 2001 by Academic Press. All rights of reproduction in any form reserved.

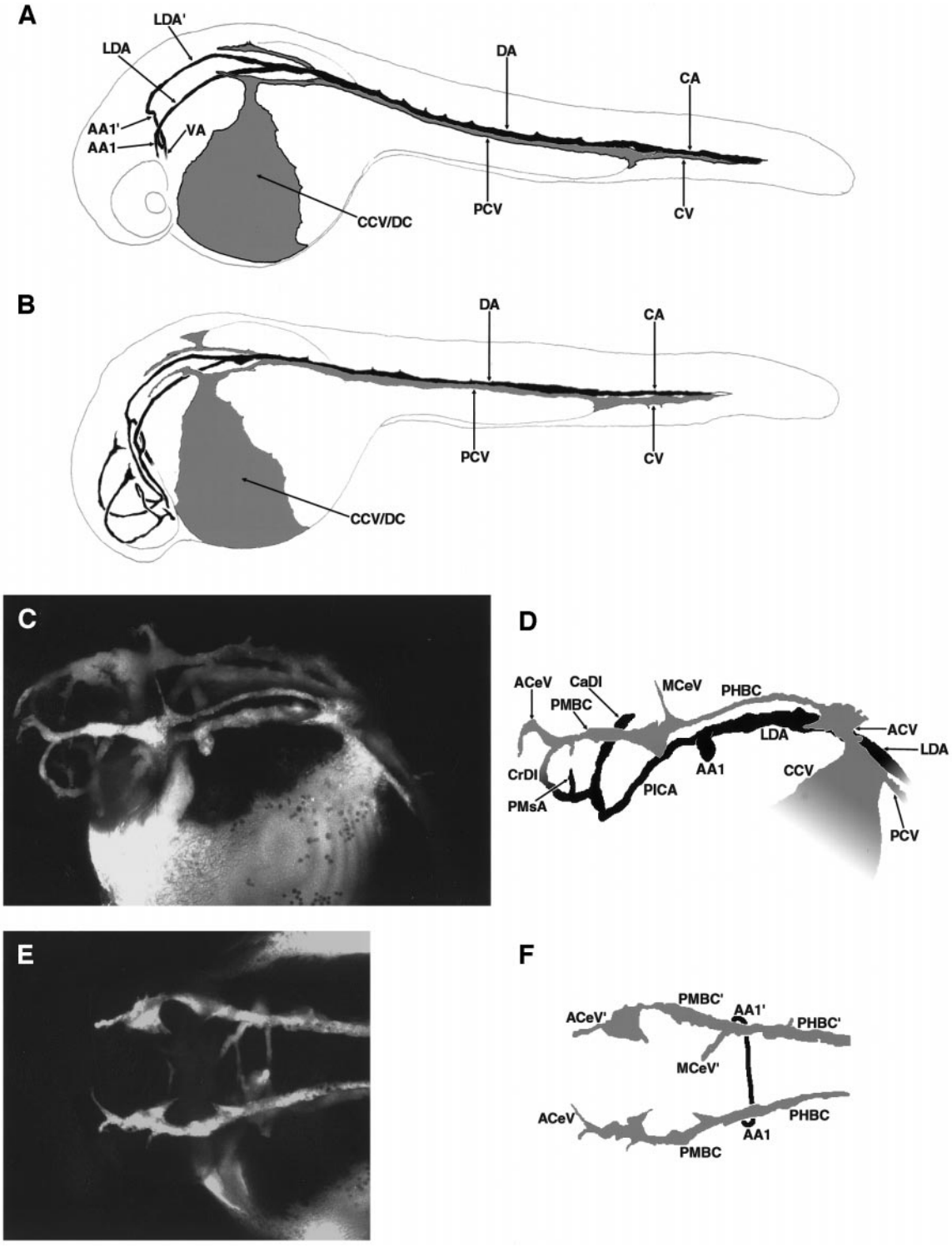

FIG. 1. Circulation in the developing zebrafish at 24–28 h postfertilization. (A) Diagram of active vessels in the zebrafish embryo just after the initiation of circulation, at approximately 24 h postfertilization (hpf). A single circulatory loop is present passing obligatorily through the trunk tail. (B) Diagram of active vessels in the zebrafish embryo a short time later, at approximately 26 hpf. A second cranial circulatory loop is now present. The stages in (A) and (B) are depicted using drawings because the weak circulation at these stages makes acquisition of attractive angiographic images difficult. These patterns are, however, representative of those seen in angiograms.

Copyright © 2001 by Academic Press. All rights of reproduction in any form reserved.

Some reticular anastomotic vessels begin to appear between the right and left DLAVs in the tail region, but not further rostrally at this stage (see Fig. 3A). In the most rostral trunk the Se and DLAV are still not active. The trunk axial vessels (DA and PCV) are relatively unchanged from their appearance at 1–1.2 dpf.

In addition to the mandibular arch (AA1), a vestigial hyoid arch (AA2) appears on either side (Figs. 2B and 2C). The radix of the LDA, where the right and left LDA merge together to form a single midline dorsal aorta which continues into the trunk, can be clearly seen (Figs. 2F and 2G). This junction point occurs at approximately the same A–P level where the ACV and PCV merge together laterally to either side into the CCV (or "duct of Cuvier," DC). The right and left CaDI extend further caudalward from the BCA as posterior communicating segments (PCS) along the base of the midbrain and merge to the single basilar artery (BA; Figs. 2F and 2G). Although the circle of vessels comprising the BCA and PCS resembles the so-called circle of Willis of humans, these are not homologous to one another. The BCA does not correspond to the anterior communicating artery of the mammalian circle of Willis, which connects the anterior cerebral arteries. The metencephalic arteries (MtA) branch dorsally from both sides of the PCS, looping up to join with the opposite MtA as well as with both MCeV at the dorsal midline of the head (dorsal midline junction, DMJ; Figs. 2F and 2G). The mesencephalic veins (MsV) sprout rostrally from this junction point as well. The BA extends caudally along the base of the medulla oblongata. Initially this vessel is unbranched but by late 1.5 dpf capillaries have begun to form connecting the BA to the two PHBC running lateral and parallel to the BA on the ventral surface of the medulla oblongata (Figs. 2F and 2G). The BA does not continue into the trunk at this stage but terminates near the end of the medulla oblongata.

The optic artery (OA) branches from the PICA at 1–1.2 dpf and enters the eye ventrally through the optic fissure as the hyaloid artery (Figs. 2D and 2E). Initially it then forms a single loop and exits the optic fissure as the hyaloid vein, continuing to the PHBC as the optic vein by 1.3 dpf. The portions of the optic vessels internal to the eye are called the hyaloid vessels, while the external portions are called the optic vessels. A new vessel, the primitive prosencephalic artery (PPrA), branches from the CrDI shortly after it exits the PICA. It extends laterally around the rostral end of the head, looping around to link to the equivalent PprA′ vessel from the other side of the embryo, and to both ACeVs, at the rostral cranial midline. The root of the PPrA becomes disconnected from the CrDI very shortly after it comes on line (Figs. 2B–2E). At or slightly after this time the PPrA, now called the prosencephalic artery (PrA), becomes instead connected to and fed by the anterior mesencephalic central artery (AMCtA) and also by the palatocerebral artery (PLA), via a communicating vessel (CMV). The AMCtA and PLA are described further below (see the "2 day" description in the next section). Another new vessel, the primitive mesencephalic artery (PMsA), branches dorsally from the CrDI, then curves caudally along the dorsal–medial wall of the eye capsule to drain into the PMBC just rostral to the midbrain–hindbrain boundary (Figs. 2B and 2C). At later stages of development the PMsA becomes disconnected from the PMBC and drains via an alternate route. The remaining part of PMsA will be used by midbrain central arteries as their drainage into the PMBC–PHBC junction (see 2 dpf description). Additional new branches from the CrDI, the palatocerebral artery (PLA) and the nasal ciliary artery (NCA), appear somewhat later, at 1.5–2 dpf (Figs. 2D and 2E). The NCA bifurcates as it almost reaches the lens in the next stage (Figs. 2D, 2E, and 3D–3G). The dorsal branch from the NCA becomes the dorsal ciliary vein (DCV) and drains into the PMBC or the PMBC–PHBC junction. The ventral branch from the NCA empties via the optic vein. Portions of both of these NCA branches are later part of the completed inner optic circle (IOC; for example see Fig. 4A). The PLA branches off ventrally from the CrDI shortly after it exits the PICA (Figs. 2D and 2E). It extends rostrally along the base of mid- and forebrain, then loops to meet the PLA′ from the other side of the embryo at the "PLA junction" (PLAJ; see Figs. 3D, 3E, and 2 dpf text for further information). The wiring pattern of the cranial vasculature and changes that occur in this pattern between 1.5 and 2 dpf are diagrammed in Fig. 14A.

2 Days Postfertilization

By 2 dpf, most trunk and tail Se have lumenized (visible by angiography) and possess an active circulation (Fig. 3A). The DLAVs are still two paired vessels cranially, but caudally many anastomotic vessels are present between the right and left DLAVs. The trunk axial vessels (DA, PCV) are still relatively unchanged from earlier stages. Over the course of the next week the CV plexus becomes gradually remodeled down to a single, better-defined vascular tube. In the cranial trunk, vascularization of the pronephric glomus begins immediately ventral to the DA just caudal to its radix. The left paired PCV has begun a process of regression

(C) Angiogram of the head of a developing zebrafish at approximately 28 hpf. Dorsal–lateral view. (D) Diagram of vessels in (C). Only the vessels on the left side are shown, for simplicity. The major, primary arterial and venous vessels of the head are visible. (E) Angiogram of the head of a developing zebrafish at approximately 28 hpf. Dorsal view. Only the major primary venous vessels (PMBC, PHBC) are visible. The primary arterial vessels (LDA, PICA) are present but are directly underneath and obscured by the PMBC and PHBC in this view. (F) Diagram of vessels in (E). All panels are oriented with rostral to the left, and all lateral views are from the left side. A glossary of the names corresponding to all labeled vessels is provided in Table 1.

Copyright © 2001 by Academic Press. All rights of reproduction in any form reserved.

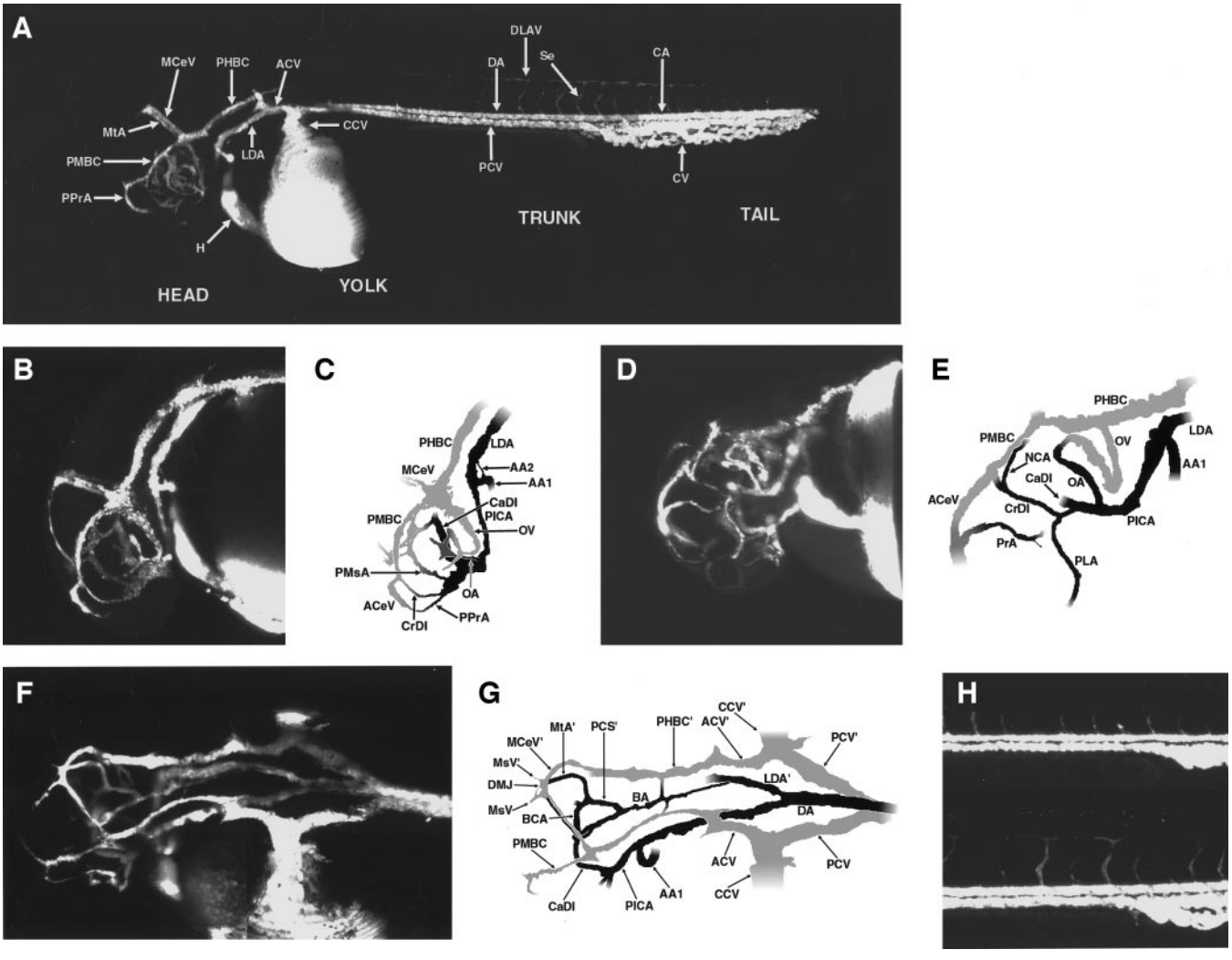

FIG. 2. Circulation in the developing zebrafish at 1.2–1.5 days postfertilization (dpf). (A) Angiogram of a developing zebrafish at approximately 1.5 dpf, compiled from two separate reconstructions pasted together. Lateral view. (B) Angiogram of the head of a developing zebrafish at approximately 1.3 dpf. Lateral view. (C) Diagram of vessels in (B). Only the vessels on the left side are shown. (D) Angiogram of the head of a developing zebrafish at approximately 1.5 dpf. Ventral–rostral–lateral view. (E) Diagram of vessels in (D). Only the vessels on the left side are shown. (F) Angiogram of the head and cranial trunk of a developing zebrafish at approximately 1.5 dpf. Dorsal–lateral view. (G) Diagram of vessels in (F). (H) Angiogram of the caudal trunks of developing zebrafish at approximately 1.2–1.5 dpf. Lateral views. The emergence of the intersegmental (intersomitic) vessels of the trunk is shown. The upper angiogram shows a somewhat earlier stage than the lower angiogram. All lateral views are from the left side. A glossary of the names corresponding to all labeled vessels is provided in Table 1.

that will continue over the next several days with the right PCV eventually carrying the venous return from almost all of the trunk and the left PCV draining only the first few SeV. The supraintestinal artery (SIA) and the subintestinal veins (SIV), which will eventually provide blood supply to the digestive system, begin to appear at or after this stage (see Fig. 4A). The SIA is a continuation of the anterior mesenteric artery (AMA), which branches out from the DA just caudal to the pronephric glomus. Visualization of the AMA and SIA by fluorescent angiography is difficult because of the position of these vessels branch deep in the ventral trunk adjacent to the yolk ball. However, they are well visualized in Berlin-blue dye-injected embryos (see Fig. 6F and 2.5 dpf text). The SIV drains directly into the PCV and CCV at this stage. At later stages the hepatic sinusoid will be interposed between the SIV and CCV/PCV.

In the aortic arch system, the third and the forth aortic arches appear around 2 dpf, and the fifth and the sixth arches develop by 2.5 dpf (see Figs. 4C–4F for intermediate and "final" stages of arch emergence, and Figs. 6B, 6D, 6E

Copyright © 2001 by Academic Press. All rights of reproduction in any form reserved.

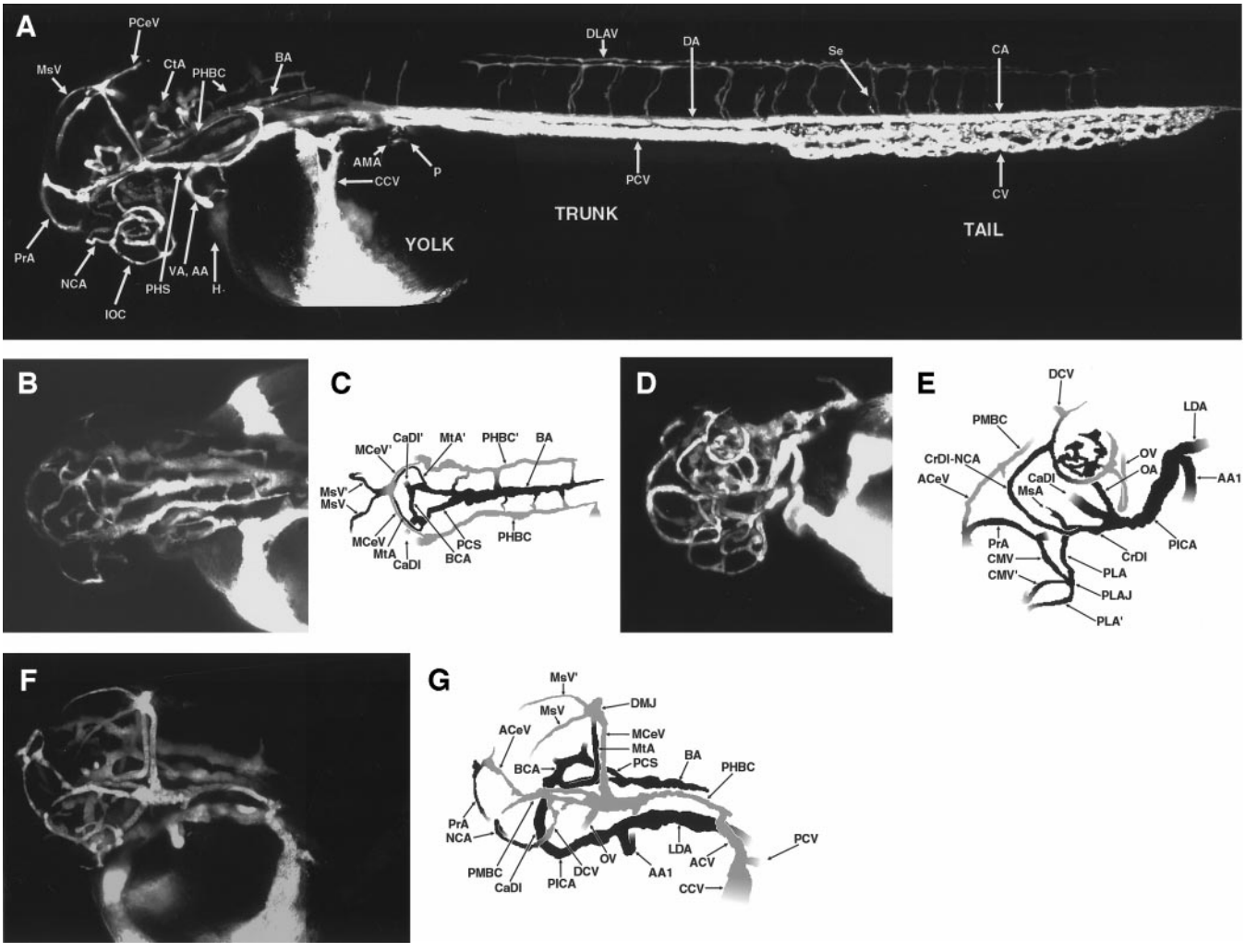

FIG. 3. Circulation in the developing zebrafish at approximately 2 days postfertilization (dpf). (A) Angiogram of a developing zebrafish at approximately 2 dpf, compiled from three separate reconstructions pasted together. Lateral view, labeled. (B) Angiogram of the head of a developing zebrafish at approximately 1.8 dpf. Dorsal view. (C) Diagram of vessels in (B). Vascular connections are apparent between the BA and both PHBC. (D) Angiogram of the head of a developing zebrafish at approximately 2.0 dpf. Ventral–rostral–lateral view. (E) Diagram of vessels in (D). Only the vessels on the left side are shown, for clarity. Note that the PPrA has now disconnected from the CrDI and the PMsA has disconnected from the PMBC. (F) Angiogram of the head of a developing zebrafish at approximately 2.0 dpf. Dorsal–lateral view. The vessels shown are mostly those on the left side, for clarity. The major arterial and venous pathways of the head at this stage are apparent. (G) Diagram of vessels in (F). All panels are oriented with rostral to the left, and all lateral views are from the left side. A glossary of the names corresponding to all labeled vessels is provided in Table 1.

and 8B–8E for more details on arch anatomy). The second or hyoid aortic arch disappears and is replaced by a more superficial vessel, the opercular artery (ORA). A new venous vessel, the primary head sinus (PHS), begins to extend rostrally from the rostral tip of the ACV along the ventral–lateral wall of the otic capsule, joining to the rostral end of the PHBC. It is generally complete before 2.5 dpf (see below). The PHS is also called the "lateral head vein" (in contrast to the "medial head vein," or PHBC; see Figs. 3A and 4C–4F). The PHS becomes the main route for venous drainage from the head, subsuming in large part the early role of the PHBC.

The main arterial route for the brain, consisting of PICA, CaDI, and BA, becomes robust by 2 dpf, and new branches appear from these vessels (Figs. 3B–3G, Fig. 14A). The OA now feeds into a small plexus of vessels within the optic cup derived from the hyaloid artery and vein (Figs. 3D and 3E). A vessel circles the rostral half of the inner rim of the optic capsule, which will at later stages be part of the completed ring of the inner optic circle. The IOC drains

Copyright © 2001 by Academic Press. All rights of reproduction in any form reserved.

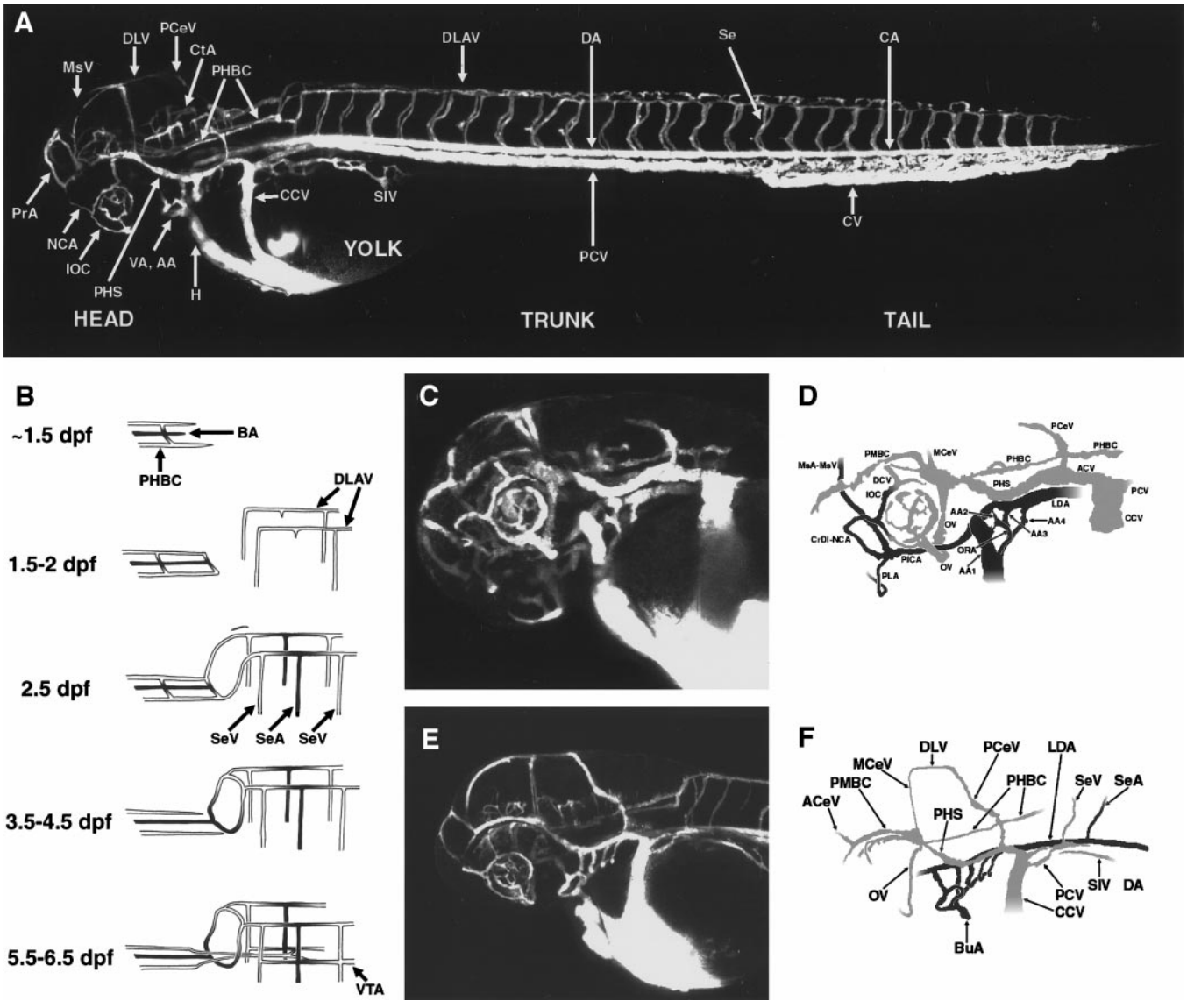

FIG. 4. Circulation in the developing zebrafish at approximately 2.5 days postfertilization (dpf). (A) Angiogram of a developing zebrafish at approximately 2.5 dpf, compiled from three separate reconstructions pasted together. Lateral view, labeled. (B) Schematic diagram showing vessels of the caudal head and cranial trunk, how these vessels become connected, and how this changes over the course of several days. (C) Angiogram of the head of a developing zebrafish at approximately 2.5 dpf. Ventral–lateral view. (D) Diagram of vessels in (C). Only the vessels on the left side are shown, for clarity. AA1–AA4 have formed, and the PHS is now on line. (E) Angiogram of the head of a developing zebrafish at approximately 2.5 dpf. Lateral view. (F) Diagram of vessels in (E). Only the vessels on the left side are shown, for clarity. All six aortic arches are now carrying blood flow. All panels are oriented with rostral to the left, and all lateral views are from the left side. A glossary of the names corresponding to all labeled vessels is provided in Table 1.

ventrally into the OV and dorsally into the DCV (Figs. 3D–3G). The vascular connection allowing the CrDI to drain directly into the PMBC has now been severed, and all of its circulation is routed through the NCA. The connection between the PMsA and the PMBC also becomes severed. The distal portion of the PMsA drains the midbrain central arteries into the PMBC-PHBC junction (Fig. 14A). The proximal portion of the PMsA becomes designated the mesencephalic artery (MsA). At slightly later stages the MsA will traverse the entire D-V extent of the head to drain via the MsV into the dorsal longitudinal vein (DLV; see Figs. 5A–5D, tracing the course of MsA through panels). At this stage, however, the MsA does not yet connect to the MsV (Figs. 3D–3G). PLA extends rostrally from CrDI along

Copyright © 2001 by Academic Press. All rights of reproduction in any form reserved.

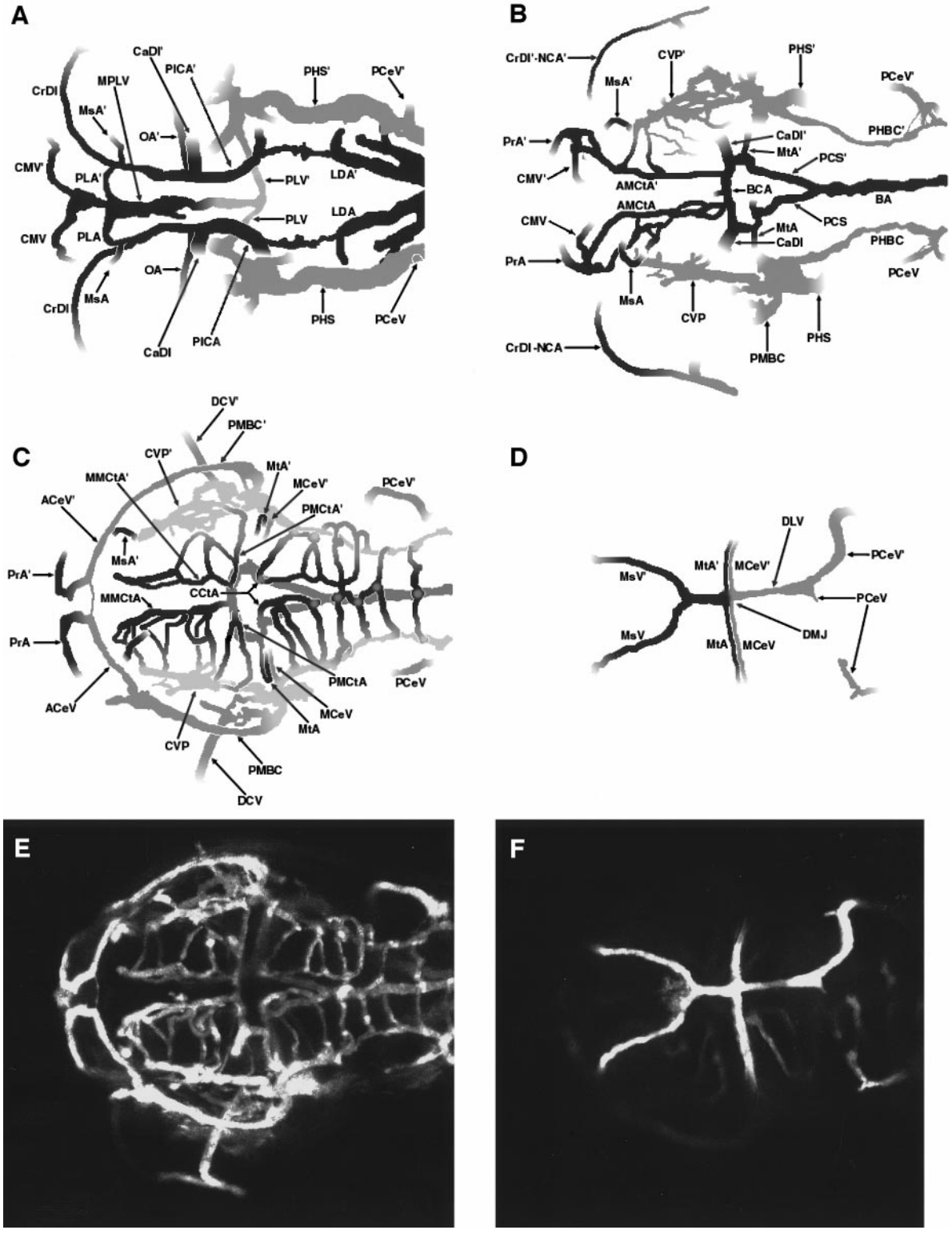

FIG. 5. Multilayer composite diagram of circulation in the developing zebrafish head at approximately 2.5 days postfertilization (dpf). A 2.5 dpf dorsal–view angiographic image stack was divided into 4 substacks and each substack was separately reconstructed. Drawings were prepared detailing the vascular patterns in each of these reconstructions. (A) Bottom layer diagram, showing ventral cranial vessels (beginning approximately just above the future pharynx). (B) Lower middle layer diagram. (C) Upper middle layer diagram. (D) Top layer diagram, showing the most dorsal cranial vessels. (E) Angiogram corresponding to the diagram in panel (C). (F) Angiogram corresponding to the diagram in panel (D). All panels are oriented with rostral to the left and left down. A glossary of the names corresponding to all labeled vessels is provided in Table 1.

Copyright © 2001 by Academic Press. All rights of reproduction in any form reserved.

the base of mid- and forebrain, then loops medially and links to the corresponding vessel from the other side of the embryo (PLA′) at the PLA junction (PLAJ). Two new vessels, the communicating vessels CMV and CMV′, branch dorsal–laterally from the PLAJ, and link to the base of PrA or PrA′ (Figs. 3D, 3E, 5A, 5B, and 14A). Another new vessel also appears at or slightly after this stage, the median palatocerebral vein (MPLV). It takes off in a caudal direction from the midpoint of the PLA–PLA′ loop and proceeds straight caudally along the cranial midline just above the pharynx, just below the diencephalon (third ventricle). At a level just caudal to the eye it ends in a T, and its two branches, the palatocerebral veins (PLV) each drain laterally into the OV, and from there to the PMBC-PHBC junction (Figs. 5A, 7A, and 14A).

At this stage, a number of central arteries (CtA) also begin to penetrate into the brain substance (Figs. 3A, 5, and 14A). Three pairs of CtA extend from the BCA to irrigate the fore- and midbrain. The anterior mesencephalic central arteries (AMCtA), AMCtA and AMCtA′, extend rostrally. The PrA branch ventrally from the AMCtA, then irrigate the forebrain, draining via the ACeV and eventually into the PMBC (Fig. 5B). The PLA also empties into the PrA via the CMV (Figs. 3D, 3E, 5A, 5B, and 14A). The AMCtA irrigate rostral regions of the midbrain. The middle mesencephalic central arteries (MMCtA and MMCtA′) project rostrally and dorsally to irrigate the midportion of the midbrain (Figs. 5C and 14A). Another pair of CtA, the posterior mesencephalic central arteries (PMCtA), PMCtA and PMCtA′, project dorsally from BCA to irrigate the caudal part of midbrain (Figs. 5C and 14A). These sets of vessels can often have common roots from the BCA (for example, see AMCtA′, MMCtA, and PMCtA in Figs. 10B and 10C). Eventually the AMCtA, MMCtA, and PMCtA all drain into the PMBC-PHBC junction via the remnant of the PMsA, as noted above. Still another pair of CtA, the cerebellar central arteries (CCtA and CctA′), take off and extend upward from the PCS, branch to provide an arterial feed to the hindbrain, then drain back down into the PHBC (Figs. 5B, 5C, and 14A). Many additional single central arteries extend dorsally from the BA, branch and intermingle, then loop down and drain into the PHBC (Figs. 5C and 14A). The BA and the paired PHBC extend caudally and make further interconnections on the ventral surface of the medulla oblongata. There is a prominent interconnection formed at the caudal-most end of both sets of vessels. At this same point, a connection forms at 2–2.5 dpf linking the caudal ends of both PHBC to the paired DLAVs more dorsally in the cranial trunk (Fig. 4B). Eventually, this connection will detach from the PHBC and be solely from the BA at later stages. These and other changes in the vasculature of the head–trunk junction are detailed in Fig. 4B. In the cranial vascular system, the two MsV can be seen projecting rostrally from the DMJ or DLV and then diving ventrally. These vessels will eventually link to the MsA, but as noted above are not at this stage continuous through the head (Figs. 3A, 3F, and 3G). The posterior cerebral veins (PCeV) also begin to appear at this stage, sprouting caudally from the DMJ or DLV and then eventually diving ventrally (Fig. 3A). The PCeV are also not complete at this stage; they will eventually drain into the ACV (Figs. 4E, 4F, and 5A–5D). As noted above (in the 1.5 dpf section) the wiring pattern of the cranial vasculature and changes that occur in this pattern between 1.5 and 2 dpf are diagrammed in Fig. 14A.

2.5–3 Days Postfertilization

By 2.5 dpf, the trunk and tail Se are usually all patent (Fig. 4A). The arterial–venous identity of these vessels does not follow a fixed pattern from embryo to embryo, except for the first four sets of Se, which do apparently have an invariant pattern (unpublished results; see also Discussion). Other SeV and SeA do not alternate between arteries and veins from one segment to the next, and the A-V identity of a given Se in a given segment is different from embryo to the next. The DLAVs are reticular throughout the tail and caudal half of trunk (but not in the cranial trunk). They continue to "zipper" together in a caudal to rostral progression. As noted above, by this stage of development the DLAVs are also connected to the PHBC and BA in the head (see Fig. 4B for an explanation of changes in head–trunk connections). Beginning at 2.5–3 dpf, a small vessel begins to extend caudally from the caudal-most end of the CA into the base of the caudal fin (Fig. 4A). Initially this vessel extends as a single tube but at later stages it splits into a pair of vessels, forming a caudal circulatory loop (Fig. 9A, for example). Increased D-V separation begins to appear between the axial vessels (DA and PCV), a process that will continue at least through 4.5 dpf. The CV plexus continues to slowly condense down into a single more ventral channel.

The large CCV or duct of Cuvier is narrow and moves to a more cranial position as it fans out across the yolk ball (Fig. 4A). The right PCV continues to become more dominant, now carrying most of the venous return from the trunk, whereas the left PCV drains primarily SeV from only the first 1–4 segments (Figs. 4E and 4F). At approximately 2.5–3 dpf a new sprout also takes off caudally from the AMA just after it exits the DA. This vessel is the arterial branch to the swim bladder (SBA). The AMA continues on to become the SIA (see Fig. 6F). Several (2–4) posterior mesenteric arteries (PMA) branch ventrally from the DA and anastomose longitudinally along the dorsal wall of the hindgut, forming the caudal part of the SIA (these vessels, and the SIA, are not well visualized in most of our angiograms). The cranial portion of the SIA extends caudally from the AMA and joins to the caudal SIA of hindgut, completing the full extent of the SIA (reasonably well visualized in Fig. 8A and diagrammed in Fig. 14B). The AMA and its branches and connections are detailed further in the next section and in Fig. 6F. The vascular plexus of the mid- and hindgut walls also appears by 3 dpf. The right and left SIV, which drain this plexus, are by 3 dpf continuous across most of the dorsal–lateral aspect of the yolk ball (Fig.

Copyright © 2001 by Academic Press. All rights of reproduction in any form reserved.

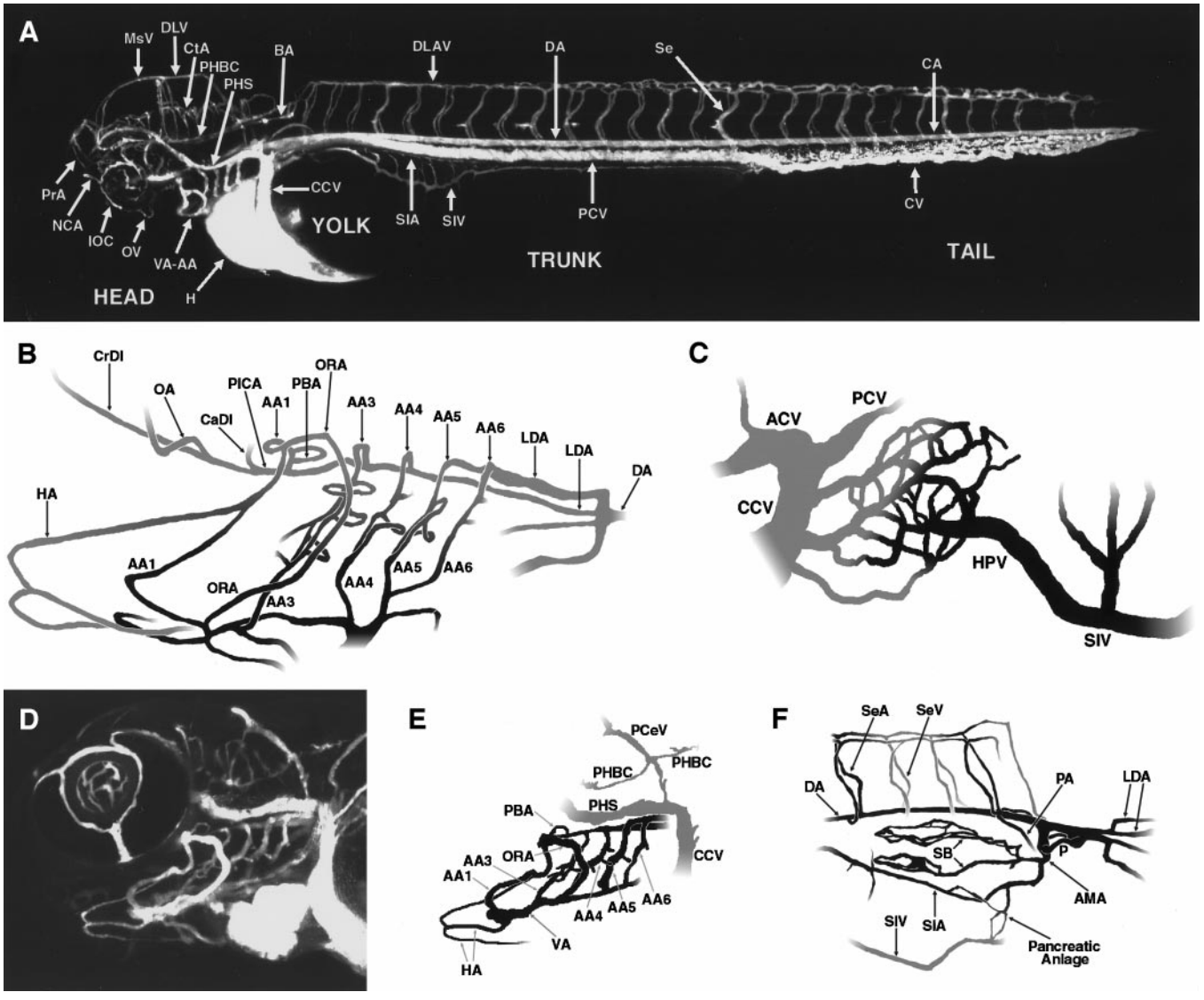

FIG. 6. Circulation in the developing zebrafish at approximately 3–3.5 days postfertilization (dpf). (A) Angiogram of a developing zebrafish at approximately 3.5 dpf, compiled from four separate reconstructions pasted together. Lateral view, labeled. (B) Schematic diagram illustrating how the aortic arches feed into the ventral cranial arterial circulation, prepared from a Berlin-blue dye-injected 3.5 dpf specimen. Note that the caudal two aortic arches (AA5 and AA6) empty into a separate branch of the lateral dorsal aorta. (C) Diagram showing the renal vascular plexus and associated vessels that feed and drain the liver, at 3.5 dpf. (D) Angiogram of the head of a developing zebrafish at approximately 3 dpf. Ventral–lateral view. (E) Diagram of vessels in (D). Only the aortic arches, associated arterial vessels, and a few of the major venous vessels seen in (C) are depicted in the diagram. Note the appearance of the HA, and elongated VA, and vascular sprouts appearing on AA3–AA6. (F) Diagram showing the anterior mesenteric artery and its branches in the ventral cranial trunk at 3 dpf, prepared from a Berlin-blue dye-injected 3.5 dpf specimen. All panels are oriented with rostral to the left, and all lateral views are from the left side *except* for (F), which is a right-side view with rostral to the right. A glossary of the names corresponding to all labeled vessels is provided in Table 1.

14B), although they are not always continuous over the yolk extension at 2.5–3 dpf (compare Figs. 4A and 6A). The most rostral end of the left SIV begins to divide into separate smaller channels. These numerous elaborating branches represent the forming reticular hepatic sinusoids (see Figs. 4A and 6C for a diagram of liver vascularization at 3.5 dpf). Just caudal to this, the most rostral unbranched portion of the left SIV will become the hepatic portal vein. Multiple venous connections (hepatic veins) appear linking the forming reticular hepatic sinusoids to the left

Copyright © 2001 by Academic Press. All rights of reproduction in any form reserved.

PCV and CCV (mostly to the left CCV; see Fig. 6C), draining blood from the developing liver. At the caudalmost end of both SIVs some minor drainage routes also form from these vessels to the PCV. The pectoral (subclavian) artery (PA) and pectoral vein (PV) come on line at late 2.5 to 3 dpf. The PA takes off directly from the lateral wall of the DA caudal to the pronephric glomus, at the same level as the root of the second SeA (see Fig. 6F). The PV drains into the ACV just cranial to its junction with the CCV (see 4 dpf section and Fig. 9C for diagram of pectoral vessels).

Despite massive elaboration of smaller caliber vessels in the head through 7 dpf (the latest stage examined in this study), the overall wiring pattern of major head vessels is largely unaltered after 2–2.5 dpf. There are a few significant changes at this stage, however. With the development of the fifth and the sixth aortic arches, the complete set of aortic arches is generally present by 2.5 dpf (see Figs. 4C–4F for intermediate and final stages of arch formation). The connections between the aortic arches and the cranial circulatory system are detailed more fully in the next section (see Fig. 6B). The caudal two aortic arches (AA5 and AA6) drain by a common route into a separate, more superficial branch of the LDA (Fig. 5A). This separate branch flows to the radix of the dorsal aorta in the cranial trunk, and AA5 and AA6 eventually are the major (if not sole) aortic arches supplying the trunk and tail circulation (Figs. 6B, 7A). AA3 and AA4 flow into the more medial original LDA. Blood from the medial LDA flows into both the PICA and the radix of the aorta at this stage (Fig. 6B), but at later stages flows almost entirely into the PICA (Fig. 10A). Thus, AA3 and AA4 become the major aortic arches supplying the cranial circulation. The ventral aorta is now prominent (Figs. 4E and 4F), but has not yet shifted rostrally and lengthened (see Figs. 6D and 6E). Before 2.5 dpf the PHS is complete through to the large PMBC–PHBC junction point (Fig. 4). The completed PHS carries most of the venous return from the head, subsuming in large part the early role of the PHBC. The branches of the PICA are basically the same as those at 2 dpf, although the MsA is now complete to the MsV, rising up through most of the D-V depth of the head continuously to the DLV (Figs. 4A, 4C, 4D, and 5A–5D). The PCeV generally become complete at or shortly after this stage, running bilaterally from the DMJ/DLV caudally and ventrally to a junction with the PHBC, and from there through a short segment to the ACV (Figs. 4C–4F and 5B–5D)

3–3.5 Days Postfertilization

The trunk and tail SE are relatively unchanged at this stage, the basic pattern having been established by approximately 2.5 dpf, as noted above. The DLAVs in the caudal trunk and tail are just beginning to form a simpler single plexiform vessel. Two additional types of trunk vessels newly sprout at about this time, extending horizontally (along the A-P axis) from some of the SE in both directions (sprouts are apparent in Fig. 6A; also see Fig. 11 for positions of these vessels in a trunk cross section at 5 dpf). The more dorsal vessel is the primordial vertebral artery (VTA). A pair of VTA form on either side of the base of the spinal cord, adjacent to the myotome. The more ventral vessel is the parachordal vessel (PAV). A pair of PAV form lateral to the notochord, adjacent to the myotome, at the level of the horizontal myoseptum. Both sets of vessels begin to sprout in the trunk at approximately 3 dpf, and in the tail at approximately 3.5 dpf. Most of these sprouts remain very short and do not begin to progress to span the somite until 4–5 dpf. D-V separation between the axial vessels (DA and PCV) continues to increase, and the CV plexus continues to slowly condense down into a single more ventral channel. Beginning at approximately 3.5 dpf, a profusion of short vessels appears in the trunk between the DA and PCV (Figs. 8A and 9A). Most of the vessels are transient and have largely disappeared by 4.5–5 dpf. The nature of these vessels is not at present understood and awaits further (histologic) analysis.

The CCV continues to narrow and move to a more cranial path as it swaths across the yolk ball. The right PCV is by now almost completely dominant, with the left PCV draining SeV from only the first 1–4 segments (Figs. 4E and 4F). The AMA and its branches in the ventral–cranial trunk are very difficult to visualize by fluorescent microangiography but more readily observed in Berlin-blue-injected specimens (Fig. 6F). As already described briefly above, the AMA takes off ventrally from the DA just caudal to the pronephric glomus (P). Paired vascular loops for the glomus are visible draining into the AMA. Shortly after it exits the DA the AMA branches into the SBA and the SIA. The SBA runs directly caudal, then branches to form the simple plexus on the right and left sides of the swim bladder at 2.5 dpf. The left plexus drains into the left subintestinal vein from its cranial end, but we have not been able to identify this connection on the right side yet. By approximately 3 dpf the plexus has elongated across the full A-P length of the swim bladder and has formed multiple loops by approximately 3.5 dpf (Fig. 6F). The SIA also continues caudally, forming numerous connections to the two SIV on either side of the gut wall (Fig. 6A). The most cranial connections on the right side represent the vessels vascularizing the pancreatic anlage on the right intestinal wall (Fig. 6F). The SIVs run cranialward along the yolk or the ventral walls of the intestine on both right and left sides where they still serve to absorb the yolk. They drain into the liver independently via separate primary hepatic portal veins (HPV). These embryonic HPV are different from the secondary hepatic portal vein that detours across the gut at the dorsal boundary between fore- and a midgut in adult vertebrates (see Discussion).

The connections between the aortic arches and cranial arteries are detailed in Figs. 6B and 6E. Although the aortic arches are in a configuration similar to that found at 2.5 dpf, sprouts first begin to appear on the caudal four aortic arches

Copyright © 2001 by Academic Press. All rights of reproduction in any form reserved.

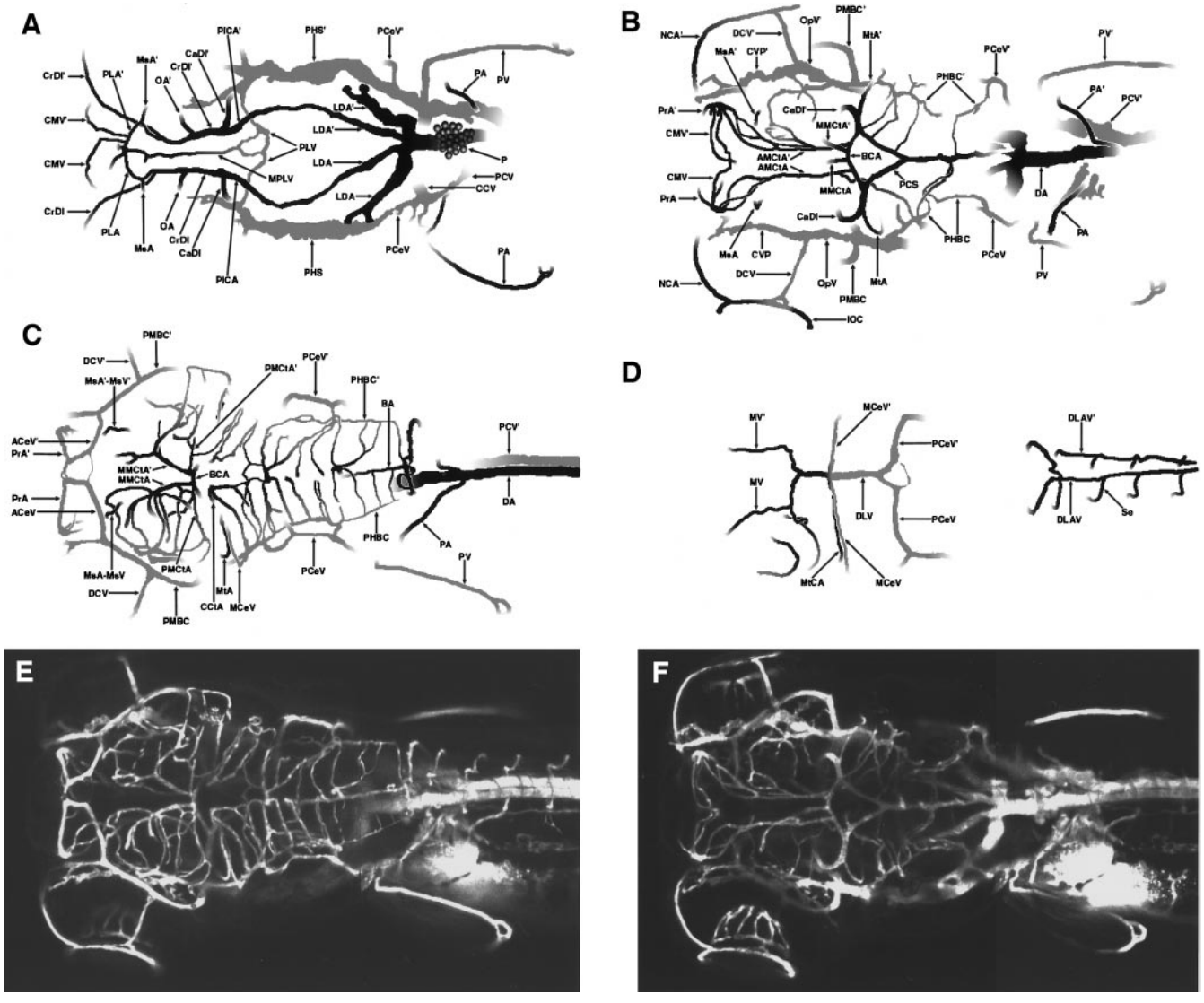

FIG. 7. Multilayer composite diagram of circulation in the developing zebrafish head and cranial trunk at approximately 3.5 days postfertilization (dpf). A pair of 3.5 dpf dorsal-view angiographic image stacks were divided into 4 paired substacks, and each of these was separately reconstructed. Drawings were prepared detailing the vascular patterns in each of the four reconstructions. (A) Bottom layer diagram, showing ventral cranial vessels (beginning approximately just above the future pharynx). (B) Lower middle layer diagram. (C) Upper middle layer diagram. (D) Top layer diagram, showing the most dorsal cranial vessels. (E) Angiogram corresponding to the diagram in panel (C). (F) Angiogram corresponding to the diagram in panel (B). All panels are oriented with rostral to the left and left down. A glossary of the names corresponding to all labeled vessels is provided in Table 1.

(AA3–AA6) at approximately 3 dpf, usually on their caudal–lateral surfaces (Figs. 6D and 6E). These sprouts will give rise to the branchial laminar arteries (ALB) of the future gills. By 3.5 dpf the third, forth, and fifth aortic arches have started to divide into afferent (proximal to the ventral aorta) and efferent (proximal to the lateral dorsal aorta) branchial arteries (ABA and ABF, respectively). This process, which proceeds in a rostrocaudal direction from AA3 to 6, continues for the next several days (see Figs. 6B, 8D, and 8E). At this stage there is still a direct connection between the end of the ABF and the ABA. By 3.5–4 dpf the vascular sprouts that first appeared at 3 dpf on the four caudal aortic arches are now starting to become short loops (Figs. 6B and 8B–8E). Eventually they will form loops with the two ends entirely disconnected, one end linked to an ABA and the other end linked to the corresponding ABF. At this stage of development, ALB sometimes still has a single "stem" proximally even if there is a loop at the distal

Copyright © 2001 by Academic Press. All rights of reproduction in any form reserved.

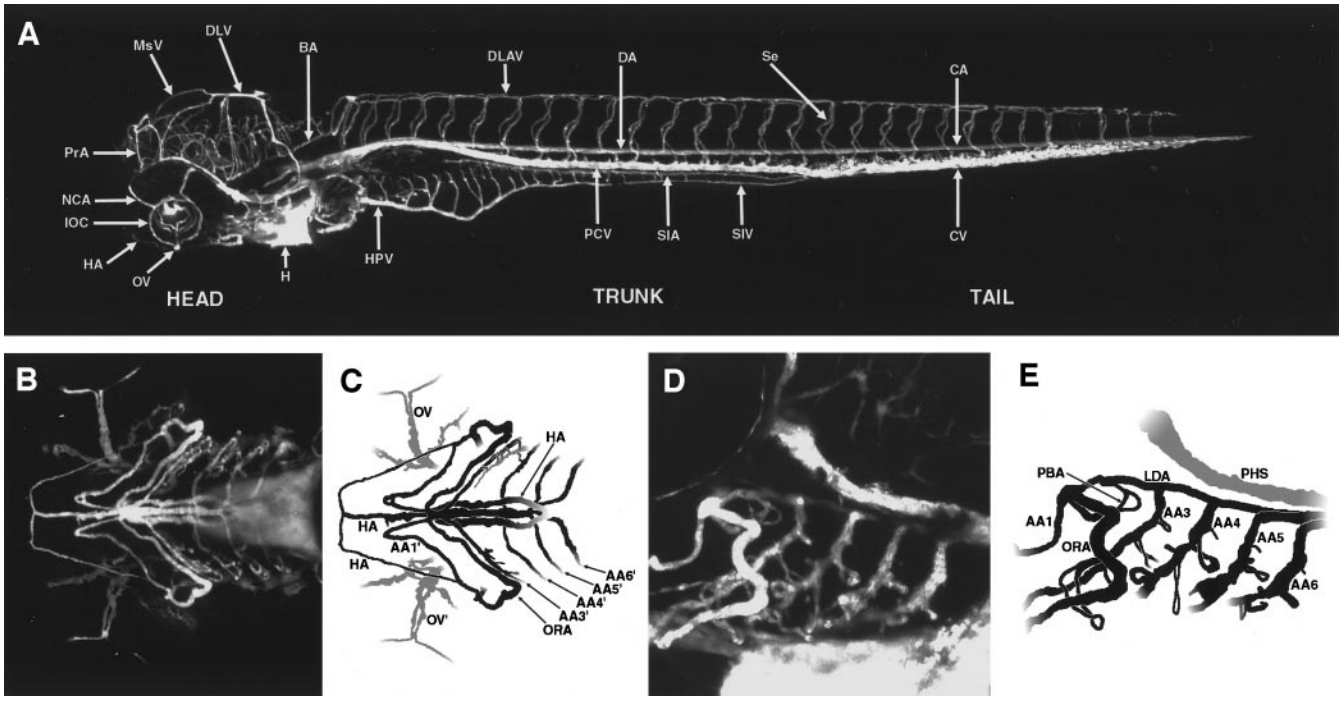

FIG. 8. Circulation in the developing zebrafish at approximately 4 days postfertilization (dpf). (A) Angiogram of a developing zebrafish at approximately 4 dpf, compiled from five separate reconstructions pasted together. Lateral view, labeled. (B) Angiogram of the ventral head of a developing zebrafish at approximately 4 dpf. (C) Diagram of vessels in (B). In this ventral view only the aortic arches and adjacent vessels are visible. All extant aortic arches are shown, as well as the hypobranchial vessels. (D) Higher magnification (20×) angiogram of the ventral head of a developing zebrafish at approximately 4 dpf. Lateral view, showing primarily aortic arches. (E) Diagram of vessels in (D). Note the vascular loops associated with AA3–AA6. Separation of these AA into parallel afferent and efferent derivatives (ABA and ABF) is in progress but not well visualized in this particular orientation of the embryo. In all panels rostral is to the left, and all lateral views are from the left side. A glossary of the names corresponding to all labeled vessels is provided in Table 1.

end. The afferent (proximal to the ABA) portion of each loop is called the afferent laminar branchial artery (ALBA) and the efferent portion (proximal to the ABF) is called the efferent laminar branchial artery (ALBE). Another new vessel associated with the aortic arches also appears at this stage, the hypobranchial artery (HA). A pair of HA are initially present, one taking off from each AA1 (Figs. 6B, 6D, 6E, 8B, and 8C). They run rostromedially until at the extreme rostro-ventral midline the two vessels merge and then run straight caudally along the ventral midline until they reach the cranial end of the VA (Figs. 8B and 8C). There, the single HA passes just dorsal to the rostral end of the VA and then immediately splits again into a pair of HA. The paired HA continue caudally just to either side of the ventral midline, passing dorsal to AA1, ORA, and AA3, and then ventral to the more caudal arches AA4, AA5, and AA6. The HA provide blood supply to the ventral branchial region and the heart.

In the cranial vascular system, the connection between the caudal end of the PHBCs and the DLAVs becomes a connection primarily to the BA during the approximately 3–4.5 dpf time period (Figs. 7C and 7D). The BA had been connected to the PHBCs at their caudal ends by 1.5–2 dpf, so this circulatory route was already present. But with the PHS coming on line and becoming the primary route for venous drainage from the head, the caudal PHBCs now drain rostrally into the PCeVs, and a vascular feed for the head–DLAV vascular link must come entirely from the BA. These changes are displayed diagrammatically in Fig. 4B. Although many additional cerebral capillaries continue to form in the head through these stages, and exiting vessels may be significantly remodeled, the basic wiring plan of major vessels established by 2.5 dpf is still maintained at this and later stages (Figs. 7, 10, and 13).

4–4.5 Days Postfertilization

In the caudal trunk and tail, DLAVs have become simpler, single plexiform vessels, while the cranial trunk DLAVs remain separate, paired, well-defined vessels (Figs. 8A, 9A, 9B, and 10D). The VTA and PAV sprouts from Se begin to progress to span the somite. By 4 dpf some of the

Copyright © 2001 by Academic Press. All rights of reproduction in any form reserved.

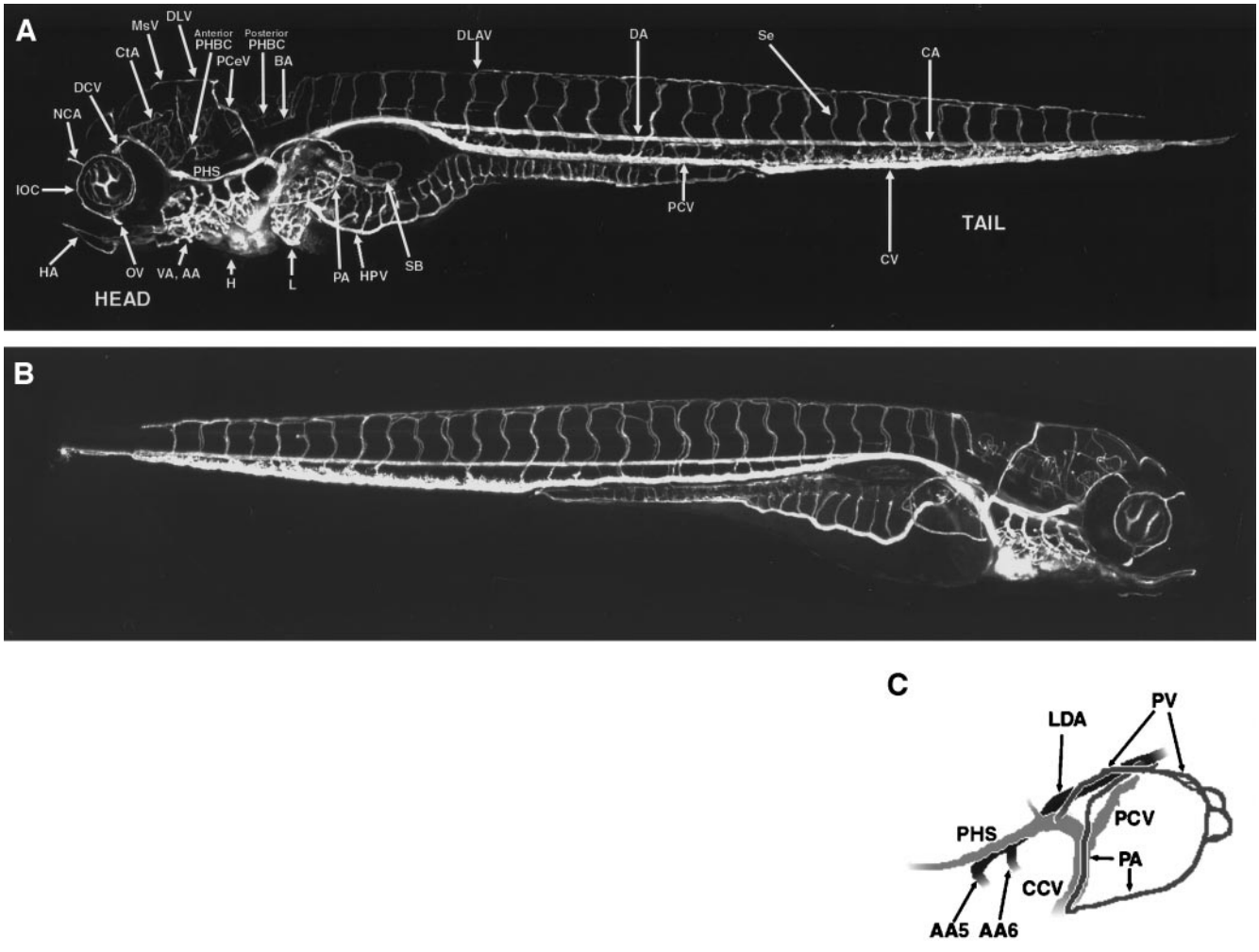

FIG. 9. Circulation in the developing zebrafish at approximately 4.5 days postfertilization (dpf). (A) Angiogram of a developing zebrafish at approximately 4.5 dpf, compiled from five separate reconstructions pasted together. Left-side lateral view, labeled. (B) Angiogram of a developing zebrafish at approximately 4.5 dpf, compiled from five separate reconstructions pasted together. Right-side lateral view, unlabeled. (C) Diagram illustrating the pectoral artery (PA) and pectoral vein (PV), and the source (from the DA) and drainage (into the ACV) of these vessels. This diagram was prepared from the angiographic stack used to generate panel (A). All panels are oriented with rostral to the left, and all lateral views are from the left side *except* for (B), which is a right-side view with rostral to the right. A glossary of the names corresponding to all labeled vessels is provided in Table 1.

VTA and by 4.5 dpf some of the PAV elongate across segments (Fig. 9A). Elongation of both longitudinal vessels continues to form additional anastomotic vessels for the nervous and trunk circulation after 7 dpf. Along the trunk, each myomere is folded in a V or chevron shape, with the point turned forward, and a horizontal septum runs fore and aft just below the tip of the cranial-pointing V's. Lateral branches (LB) sprout from the Se at the same D-V level as the PAV in the horizontal septum at approximately 4–4.5 dpf. Ventral branches from the LB begin to develop obliquely along the ventral transverse septa, forming the intercostal vessels (VI). Additional dorsal branches (DB) from the LB also appear at later stages (mostly after 7 dpf) along the dorsal transverse septa. As noted above, the positions of the DLAV, VTA, PAV, VI, and other vessels in trunk cross section are all diagrammed in Fig. 11. By approximately 4.5 dpf the increasing spatial separation of the DA and PCV, begun earlier, reaches its maximal extent. The transient short vessels developed between the DA and PCV are starting to disappear by 4.5–5 dpf. The caudal vein is continuing to remodel and condense.

The SBA now possess multiple vascular loops in which blood is actively circulating, on the ventral side of the usually partially inflated swim bladder (Fig. 6F, and poorly visualized in Fig. 8A). The right and left SIV, which are the only vessels absorbing yolk after 3.5 or 4 dpf, empty

Copyright © 2001 by Academic Press. All rights of reproduction in any form reserved.

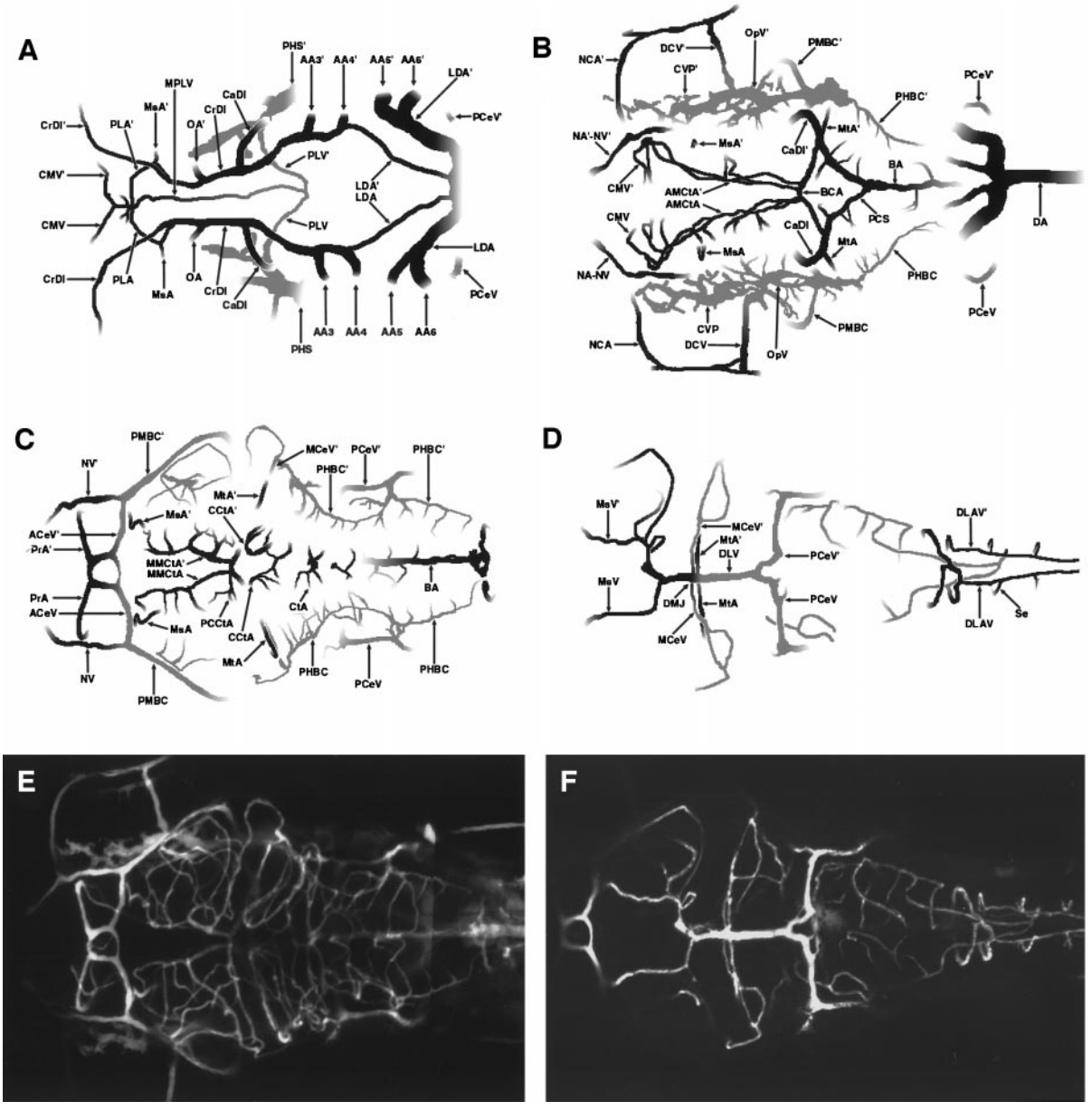

FIG. 10. Multilayer composite diagram of circulation in the developing zebrafish head and cranial trunk at approximately 4.5 days postfertilization (dpf). A pair of 4.5 dpf dorsal-view angiographic image stacks were divided into 4 paired substacks, and each of these was separately reconstructed. Drawings were prepared detailing the vascular patterns in each of the four reconstructions. For clarity, only major arterial and venous vessels and short connecting portions of smaller caliber vessels are shown in each diagram. (A) Bottom layer diagram, showing ventral cranial vessels (beginning approximately just above the future pharynx). (B) Lower middle layer diagram. (C) Upper middle layer diagram. (D) Top layer diagram, showing the most dorsal cranial vessels. (E) Angiogram corresponding to the diagram in panel (C). (F) Angiogram corresponding to the diagram in panel (D). All panels are oriented with rostral to the left and left down. A glossary of the names corresponding to all labeled vessels is provided in Table 1.

separately into the hepatic sinusoids via the two HPV at the cranial-most end of each SIV (discussed above in 3–3.5 dpf section). With the reduction of the yolk, the left SIV shows a degenerative tendency at 4 dpf. The caudal portions of the left SIV become disconnected from one another and form separate segments at 4.5 or 5 dpf (Figs. 8A, 9A, and 14B). These disconnected left caudal SIV segments will empty into the right SIV via communicating veins between the

Copyright © 2001 by Academic Press. All rights of reproduction in any form reserved.

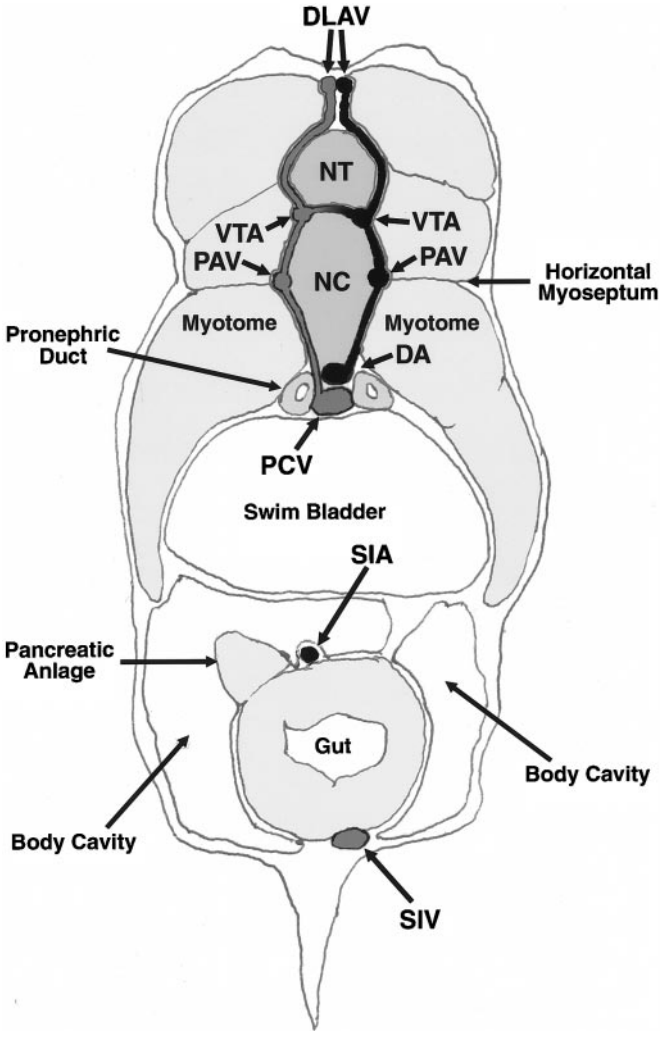

FIG. 11. Cross-sectional diagram of trunk vessels in the developing zebrafish at approximately 5 days postfertilization (dpf). The drawing was prepared by tracing a drawing of major structures in the trunk from a scanned histological section of a 5 dpf zebrafish trunk, at the A–P level of the swim bladder. The positions of extant trunk vessels were drawn in and labeled. A glossary of the names corresponding to all labeled vessels is provided in Table 1. In addition, the gut, the body cavity surrounding the gut, the pancreatic anlage, the swim bladder, one of the pronephric tubes (pronephros), the myotomes, the horizontal myoseptum, the notochord (NC), and the neural tube (NT) are all noted.

right and left SIV along the ventral gut wall (see Figs. 12 and 14B). Eventually, the remnants of the left SIV merge completely with the right SIV, and all of the venous return from the caudal gut to the liver is routed solely through the right SIV. Although the cranial-most part of the left SIV will continue to drain directly into the liver as the primary HPV, portions of the left SIV on the cranial half of midgut also degenerate, and the cranial and caudal left SIV are disconnected. The midgut itself begins to extend left-ventrad in an arch and rotates clockwise on its longitudinal axis (seen from behind) at 4 dpf. With the reduction of the left cranial SIV, a few intestinal veins newly develop on the ventral wall of midgut to empty their blood into the liver. As mentioned above, this process correlates with the reduction of yolk and the positional change of the midgut (described diagrammatically in Fig. 14B).

The parallel ABA and ABF of the third and forth aortic arches at least are completely separated from one another, and all flow from ABA to ABF becomes routed through ALB capillaries (Figs. 8B and 8C). The ALB loops are lengthening and extending further caudalward, and additional ALB loops continue to appear between the ABA and ABF in the four caudal aortic arches (Figs. 6B, 8D, and 8E). All of these changes have the effect of increasing the vascular surface area available for gas exchange in this, the future gill circulation.

In the head a pair of new arteries, the nasal arteries (NA), take off from the PICA at 4.0 dpf (see Fig. 13, also Fig. 10, although the root of the NA from the PICA is not shown in the latter figure). The NA travel rostrally, then pass along the right and left walls of the nasal sac at the most rostral end of the head. From the nasal sac, the NA flows into the nasal veins (NV). The NV rises dorsally around the front of the head, draining into the ACeV and eventually into the PMBC on either side. The NA and NV are actually the most rostrally projecting set of vessels in the embryo from this stage until at least 7 dpf. A large vascular plexus around the choroid derives from the remnant of the PMsA, which now drains the mesencephalic central arteries, as mentioned above. The DCV also drains into this plexus, which continues to elaborate adjacent to the pigment epithelium of the eye through at least 7 dpf. With the development of the choroid plexus, the ophthalmic vein separates ventrally from the remnant of the PMsA as the robust venous drainage for the plexus (Fig. 10B, more easily visualized in Fig. 13B). The PMBC, ophthalmic vein, and distal remnant of the PMsA join together further caudally at the PMBC–PHBC junction (Figs. 10A and 10B). The formation of the choroidal vascular system will be described in more detail in a later publication (S. Isogai, unpublished results).

As described earlier, blood flows in a rostral direction through the rostral PHBC, emptying into the rostral end of the PHS at the base of the MCeV (Fig. 10B). The middle and caudal segments of the PHBC drain via the PCeV (Fig. 10C). Although the portions of the PHBC draining into the PHS or PCeV have not yet completely separated from one another, they will generally do so within the next 2–3 days. The link from the extreme caudal end of the PHBC to the DLAV is no longer present, with the BA having appropriated this link (Figs. 10C and 10D). However, after 5 dpf caudal portions of the PHBC make new connections through to the trunk via vascular segments linking them to the VTA along the ventral wall of the spinal cord (Figs. 4B and 10D). In the dorsal head, the paired MsV and the two PCeV all join together into a single vessel, the dorsal

Copyright © 2001 by Academic Press. All rights of reproduction in any form reserved.

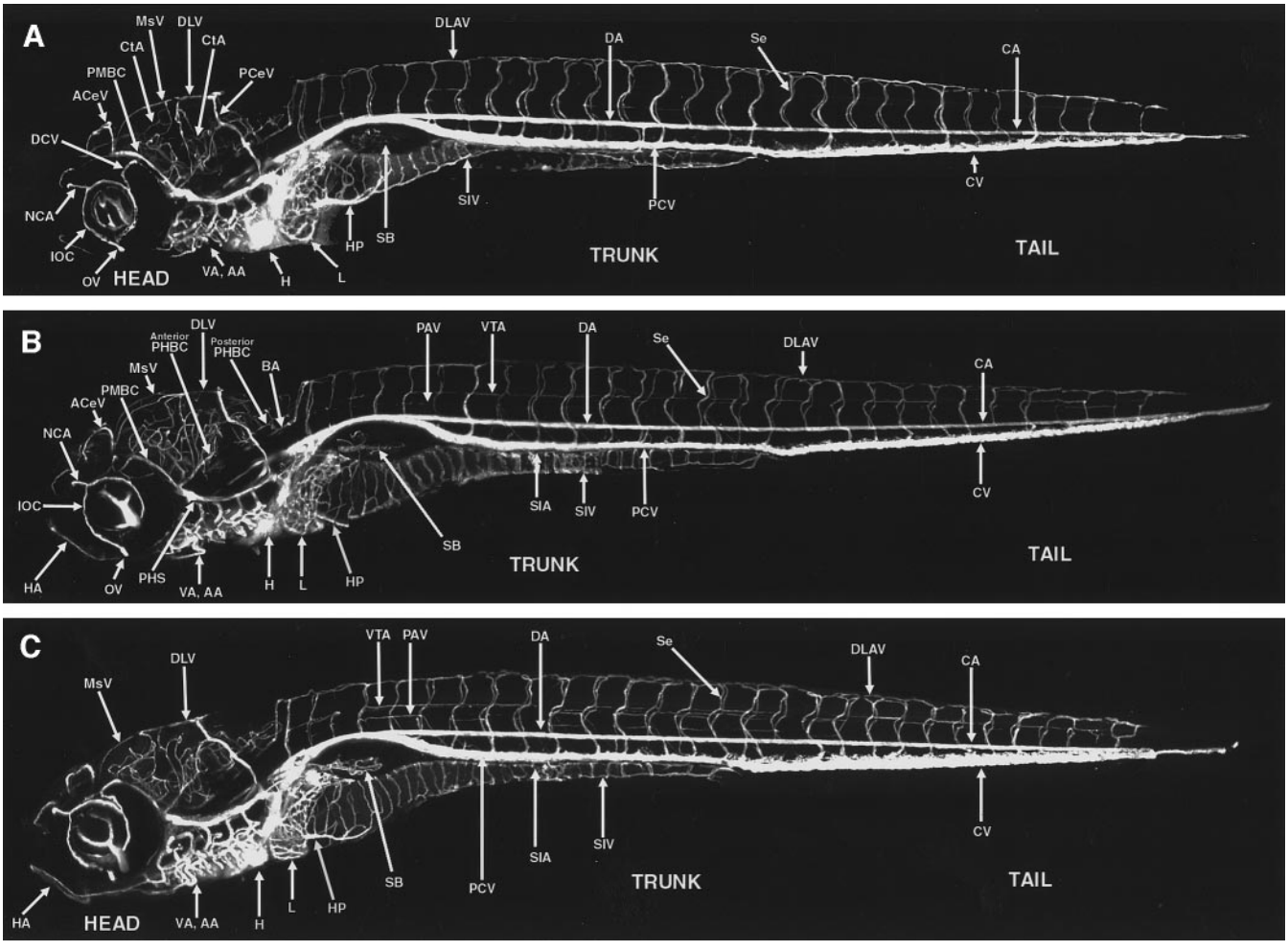

FIG. 12. Circulation in the developing zebrafish at 5.5–7.5 days postfertilization (dpf). (A) Angiogram of a developing zebrafish at approximately 5.5 dpf, compiled from five separate reconstructions pasted together. (B) Angiogram of a developing zebrafish at approximately 6.5 dpf, compiled from five separate reconstructions pasted together. (C) Angiogram of a developing zebrafish at approximately 7.5 dpf, compiled from six separate reconstructions pasted together. All panels are oriented with rostral to the left and ventral down, and particular vessels have been labeled in each panel. A glossary of the names corresponding to all labeled vessels is provided in Table 1.

longitudinal vessel (DLV) for the final portion of their length around the DMJ (Figs. 10D and 10F). Otherwise, although there continues to be an elaboration of smaller caliber vessels throughout the head, the overall wiring pattern of major head vessels is still largely the same as that seen at 2–2.5 dpf, as noted before.

5–5.5 Days Postfertilization

A single plexiform DLAV is now present throughout the caudal trunk and tail, although a pair of simple right and left DLAVs persists in the cranial-most regions of the trunk. This state is basically maintained through 7 dpf, with some additional "zippering up" of the cranial-paired DLAV vessels, moving the rostral border of the single plexiform DLAV further cranially. PAV and VTA continue to elongate across some of the segments, although in most segments these vessels still remain as sprouts (Fig. 12A). A few VI have extended ventro-caudally from the LB along the ventral transverse septa; many more can be seen by 6 and 7 dpf (Figs. 12B and 12C). The distance between the DA and PCV is no longer increasing, and the transient short vessels that had appeared between these two trunk axial vessels (DA and PCV) have by now mostly disappeared. The CV continues to remodel and condense.

With the loss of the yolk, the cranial and caudal left SIV become disconnected from one another at the hindgut, while the right SIV remains intact as the main longitudinal

Copyright © 2001 by Academic Press. All rights of reproduction in any form reserved.

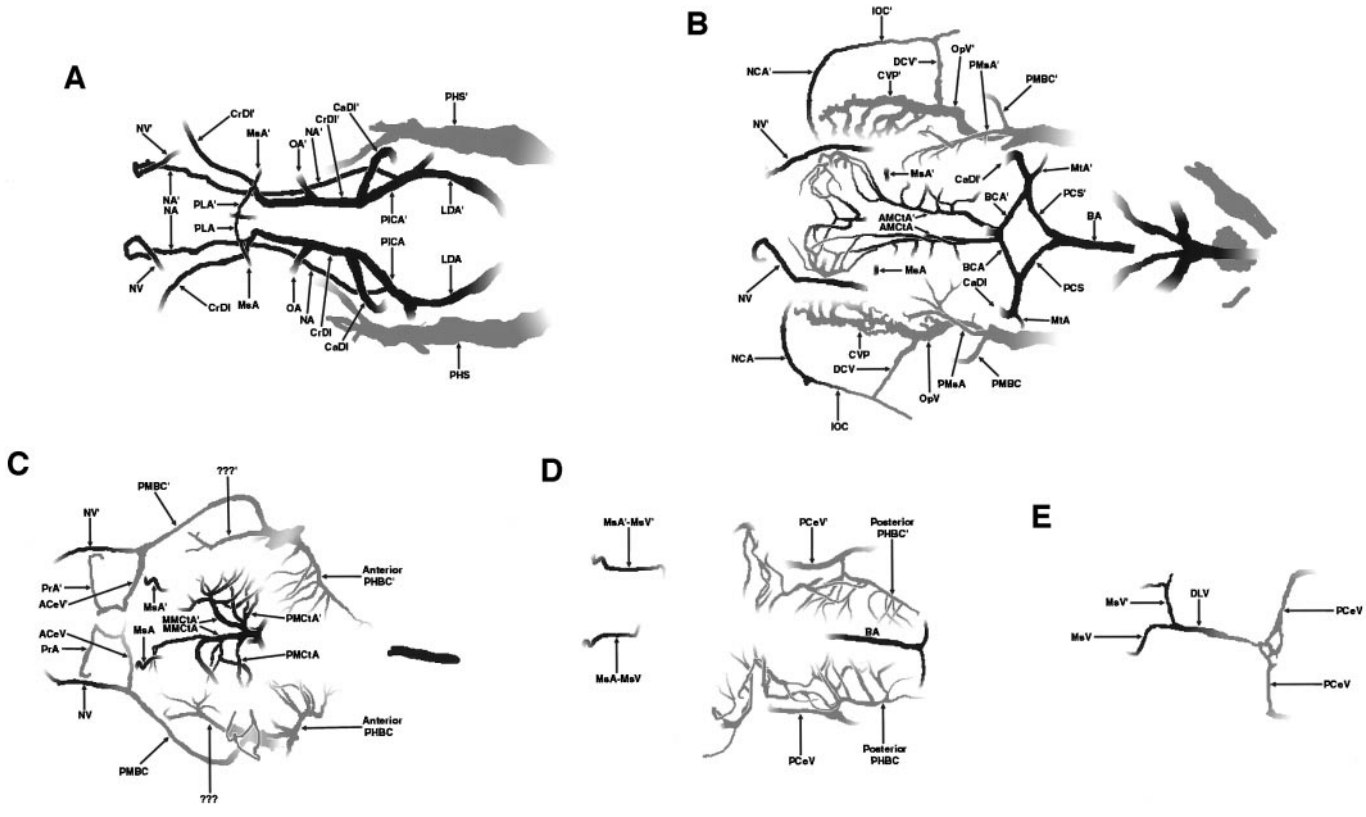

FIG. 13. Multilayer composite diagram of circulation in the developing zebrafish head and cranial trunk at approximately 6.5 days postfertilization (dpf). A pair of 6.5 dpf dorsal-view angiographic image stacks were divided into 5 paired substacks, and each of these was separately reconstructed. Drawings were prepared detailing the vascular patterns in each of the five reconstructions. These drawings are incomplete. For clarity, only major arterial and venous vessels and very portions short of the smaller caliber vessels that connect to them are shown in each diagram. Some fairly major vessels have been omitted from some drawing panels (for example, the PCeV in panels A–C). (A) Bottom layer diagram, showing ventral cranial vessels (beginning approximately just above the future pharynx). (B) Lower middle layer diagram. (C) Middle (central) layer diagram. (D) Upper middle layer diagram. (E) Top layer diagram, showing the most dorsal cranial vessels. A glossary of the names corresponding to all labeled vessels is provided in Table 1.

drainage to the liver. As a result, blood in the vascular plexus of the hindgut is forced to flow into the hepatic sinusoid via the right SIV and right HPV (except for the caudal-most portions of the left SIV, which maintain a minimal drainage to the PCV). In the cranial midgut, the remnants of the left SIV are still providing for absorption of the small amount of yolk that remains beneath the gut. A few intestinal veins that had also appeared at 4 dpf in this area extend more caudalward and drain the most ventral regions of the cranial midgut as supplementary HPVs. The SBA and its branches are actively circulating around the completely inflated swim bladder.

In the branchial arch system, the ABA and ABF are entirely separate vessels running next to one another for most of their length. The ALB continue to lengthen; additional ALB appear and some existing ALB vessels also branch to form multiple loops from a single root, although this does not begin to any significant extent before approximately 5 dpf.

Few changes in major vessels are apparent in the cranial vasculature, although many more new capillaries appear linking the major vessels. Circulation is now strong through the NA and NV. As mentioned earlier, the PHS has become the main route for venous drainage from the head, subsuming in large part the early role of the PHBC. Blood flows in a rostral direction through rostral portions of the PHBC, draining the hindbrain and rostral medulla oblongata to empty into the PMBC-PHBC junction, and from there into the PHS. The middle and caudal PHBC drain the middle and caudal hindbrain, emptying into the ventral PCeV, and from there into the ACV (Figs. 4F, 5B, 7B, 7C, and 10C). The rostral, middle, and caudal PHBC segments have continued to remodel and form numerous additional branches, and the portions of the PHBC draining into the PHS or PCeV become completely separated from one another during this stage. The elongated DLV forms a T junction, with the MsV and MsV′ branching off from the rostral T and the PCeV and

Copyright © 2001 by Academic Press. All rights of reproduction in any form reserved.

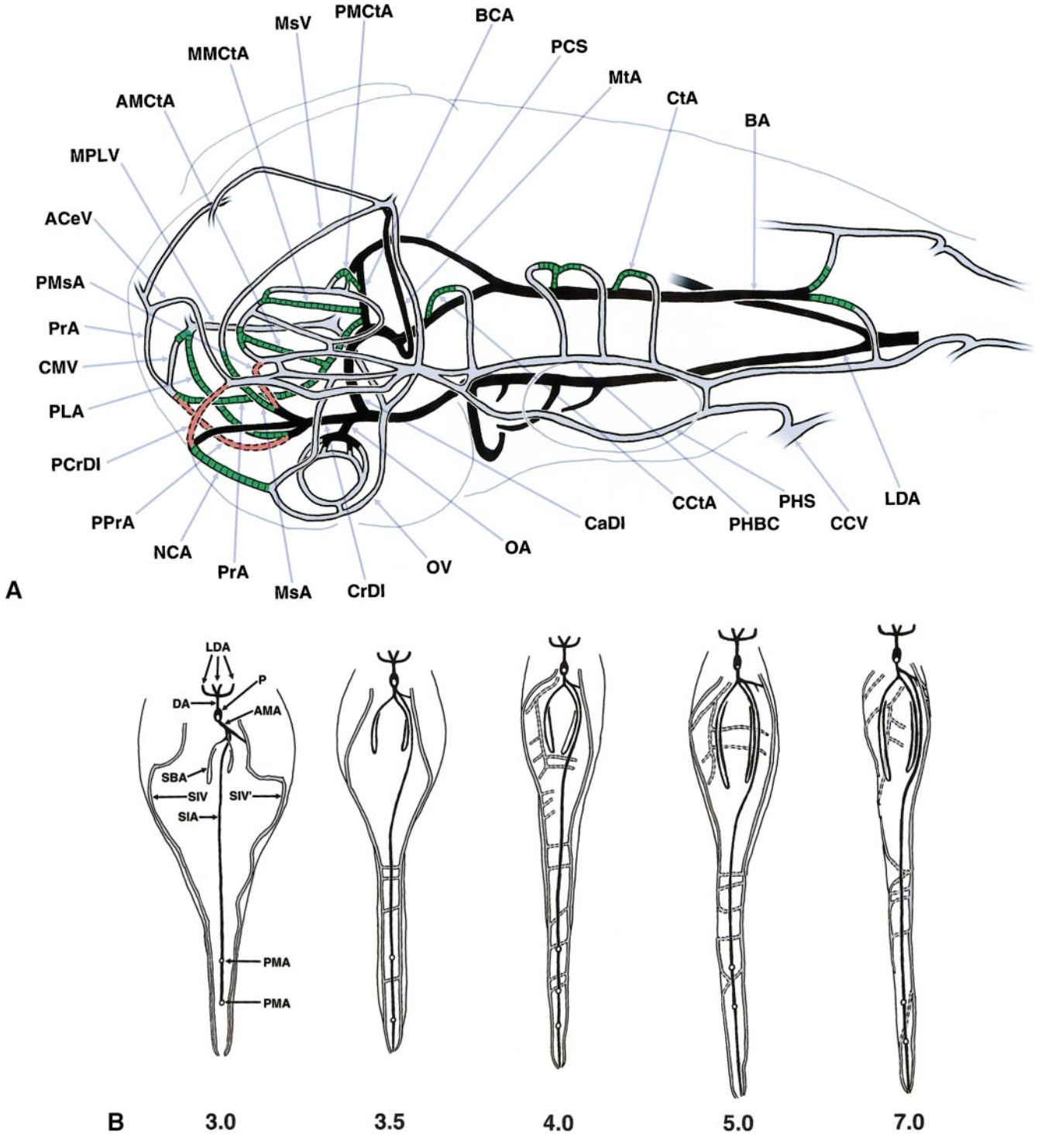

FIG. 14. Changes occurring in cranial and intestinal vessels. (A) Schematic diagram illustrating the wiring patterns of major cranial vessels from 1.2–2 dpf, and the changes that occur in this wiring pattern. This is a schematic diagram showing only the major cranial vessels, on the left side of the head; major vessels on the right side and most minor vessels have been omitted for clarity. Furthermore, while the patterns of vessel interconnections are anatomically correct, the precise positioning and/or length of different vessels may not be in perfect anatomical proportion, again in the interest of providing a clear illustration of the pattern of connections. The vessels in black are the main arterial routes for the head. Vessels in gray are either secondary arterial or venous vessels. Red-hued vessels with walls drawn with dashed lines represent vascular connections that are initially present at 1–1.5 dpf, but then later lost (early, transient pathways). Green-hued vessels

Copyright © 2001 by Academic Press. All rights of reproduction in any form reserved.

PceV′ branching off from the caudal T (see Figs. 10D and 13E).

6–7 Days Postfertilization

The basic pattern of the vasculature established during previous stages remains mostly intact. Some major vessels still remain in an incomplete state, however (Fig. 12).

In the trunk and tail, the DLAVs continue to anatomose slightly further cranially. The longitudinal VTA and PAV extend across most of the trunk segments, but some are incomplete yet. By 7 dpf many VI have extended the full D-V length of the ventral vertical septum boundary, and some dorsal branches from LB have also begun to appear along the dorsal transverse septa, although circulation is weak through these and they are poorly visualized (Fig. 12). Microscopic observations indicate that the dorsal branches have their arterial root at the dorsal tip of intersegmental arteries while the ventral intercostals have their root at the dorsal aorta. Both dorsal and ventral branches drain into the intersegmental veins at the level of the PCV.

The SBA is now an elaborate set of many looped, branched vessels on the ventral surface of the inflated swim bladder (Figs. 12B and 12C). With the complete loss of the yolk, the left cranial SIV degenerates except at its cranial-most end, which drains into the hepatic sinusoid. The separate, additionally developed intestinal veins now play a major role for the ventral territory of cranial midgut as HPVs (Fig. 14B). All of the SIVs and supplementary intestinal veins drain into the liver via the ventral midgut wall and show no sign as yet of the secondary hepatic portal vein that will presumably (as occurs in other vertebrates) later detour across the gut at the dorsal boundary between fore- and midgut.

In the branchial arch system, ALB continue to grow, proliferate, and elaborate. The further changes in these vessels have not been characterized as a part of this study. In the cranial vasculature, major vessels are relatively unchanged in their patterns of connections, but extensive remodeling and shifting of vessels, particularly smaller caliber vessels and capillaries, continue throughout this period. It should be noted that we have not observed up to this stage, and have still not confirmed the later appearance of, the direct connection between the BA and VTA that is seen in all other vertebrates (see Discussion).

DISCUSSION

An Atlas of Vascular Anatomy for the Developing Zebrafish

The genetic tractability of the zebrafish and the accessibility and optical clarity of its embryo make this a particularly useful model for genetic and experimental studies of vascular development. Mutational screens have already resulted in the identification of vascular-specific mutants (Stainier *et al.*, 1995; Weinstein *et al.*, 1995) and cloning of at least one novel vascular-specific gene (Zhong *et al.*, 2000). However, the lack of a detailed, standardized description of the normal anatomy of the developing vasculature of the zebrafish has made it difficult to fully exploit these advantages. In this paper and in an accompanying Web site online at http://eclipse.nichd.nih.gov/nichd/lmg/redirect.html, we now present a detailed wiring plan for the major vessels of the patent vascular system of the embryonic and early larval zebrafish.

We find that the formation of vascular tracts in the zebrafish follows a plan similar to that of other vertebrates (for a detailed comparative analysis of vascular development in the zebrafish and other vertebrates see "The interactive atlas of zebrafish vascular anatomy" at http://eclipse.nichd.nih.gov/nichd/lmg/redirect.html). There are of course some unique features in the vascular plan of zebrafish. As in other teleosts, most of these differences appear to be either extensions to or adaptations of the basic plan that accommodate specialized circulatory requirements. Other differences found specifically in the zebrafish may be explained on the basis of its very rapid development. Circulation begins in the zebrafish at 24 h postfertilization; eggs hatch by 2–2.5 dpf, and, with the consumption of yolk, free-swimming larvae begin feeding by approximately 5 dpf. Their rapid early development may reflect the fact that the eggs of zebrafish and many other teleosts are released directly into the water column for fertilization and are readily available to predators. The need to escape predation may create significant evolutionary pressure to accelerate the pace of development and generate a free-swimming, feeding larva in the least time possible. Whatever the cause, in at least some respects, vessel formation in the zebrafish does appear to be "stripped-down," with nonessential features eliminated in the interest of rapid development. The primary trunk vessels, the dorsal aorta and posterior cardinal vein, form rapidly and without apparent secondary angiogenic remodeling. Furthermore, some "intermediate

with hatch marks drawn across them are vascular connections or arterial roots of vascular connections that are *not* initially present at 1–1.5 dpf, but appear by 2 dpf (later emerging pathways). Many of the major vessels are labeled, with light blue arrows used to designate the particular vessel named. (B) Diagram illustrating changes in intestinal vessels between 3 and 7 days postfertilization (dpf). This is a schematic diagram showing only the major vessels. Secondary vessels (particularly those linking the main arterial and venous trunks) have been omitted for clarity. A glossary of the names corresponding to all labeled vessels is provided in Table 1.

Copyright © 2001 by Academic Press. All rights of reproduction in any form reserved.

stages" of the vascular anatomy found in other vertebrates with longer developmental periods are missing in the zebrafish. Some examples of this are the transverse vessels, the "primitive" subintestinal vein (connected to the caudal vein), and the bilateral longitudinal neural arteries (see the "Interactive atlas of zebrafish vascular anatomy" at http://eclipse.nichd.nih.gov/nichd/lmg/redirect.html).

Vessel Formation Is a Highly Dynamic Process, but It Follows a Stereotypic Program

The conserved nature of the basic vertebrate vascular plan and relative reproducibility of vessel pattern we have observed from embryo to embryo in zebrafish do not imply that vessel formation is a static, fixed process. Vessel formation in the developing zebrafish is extremely dynamic, with vessel tracts appearing and disappearing and links between vessels severing and then reconnecting in entirely new patterns. Most of these changes follow a reproducible, stereotypic plan, however. The cranial vasculature provides a particularly good example of this. Unlike previous methods, confocal microangiography of zebrafish allows easy visualization of the pathways of the central arteries that penetrate deep into the brain substance. This has given us new insights into how central cranial vessels form and how the emergence of these vessels alters the overall pattern of the vasculature. From our observations of the cranial vasculature, it is difficult to explain the impetus for many of the changes in vascular pattern solely on the basis of either the demands of local tissues for oxygen and nutrients or flow-based vessel remodeling. Figure 14A illustrates some of the changes that take place in the vessels of the zebrafish head. One example is the primitive mesencephalic artery (PMsA). This vessel, which takes off from the cranial division of internal carotid artery (CrDI), at first drains into the primordial midbrain canal (PMBC). This connection severs, and the vessel (now called the mesencephalic artery, MsA) becomes connected instead to the mesencephalic vein (MsV). Another example is the primitive prosencephalic artery (PPrA), which initially is also fed by the CrDI. This connection severs and the vessel, now the prosencephalic artery (PrA), becomes fed instead by the anterior mesencephalic central artery (AMCtA) and also by the palatocerebral artery (PLA), via the communicating vessel (CMV). In both of these examples, the primitive vessels appear to be functioning perfectly well, and there is no obvious reason for them to sever their connections and become part of an entirely different vascular pathway. In fact, in both cases rewiring actually creates longer and moretortuous circulatory circuits. We suggest that these changes are not driven primarily by altered flow dynamics or local tissue demands. We suggest instead that the major impetus for these changes comes instead from developmental patterning cues organized by specific, genetically programmed molecular pathways, in much the same way that genes and molecular cascades direct the formation of other internal organs such as the nervous system. In fact, loci necessary for patterning specific, localized regions of the vasculature have already been identified by mutational analysis in the zebrafish (Chen *et al*., 1996; Stainier *et al*., 1996). Further study of these and other vascular patterning mutants, as well as *in vivo* experimental studies in the zebrafish, should help identify these genetically programmed patterning changes and elucidate how the interplay between "hard-wired" genetic cues and local environmental cues from vascularized tissues results in the formation of the intricate vascular network.

REFERENCES

Aoyama, M. (1956). Disvolvigo de sangvazoj de la mez- kaj finintesto ce hynobius naevius. *Kaibogaku Zasshi* **31,** 573–598. [in Japanese, Esperanto summary]

Chen, J. N., Haffter, P., Odenthal, J., Vogelsang, E., Brand, M., van Eeden, F. J., Furutani-Seiki, M., Granato, M., Hammerschmidt, M., Heisenberg, C. P., Jiang, Y. J., Kane, D. A., Kelsh, R. N., Mullins, M. C., and Nusslein-Volhard, C. (1996). Mutations affecting the cardiovascular system and other internal organs in zebrafish. *Development* **123,** 293–302.

Colle-Vandevelde, A. (1963). Blood anlage in teleostei. *Nature* **4886,** 1223.

Disler, N. N. (1957). Development of the chum salmon of the Amur river *Oncorhynchus keta* (Walb). *Trudy. Inst. Morph. Zhiv. Severtsova* **20,** 3–70. [in Russian]

Driever, W., Solnica-Krezel, L., Schier, A. F., Neuhauss, S. C., Malicki, J., Stemple, D. L., Stainier, D. Y., Zwartkruis, F., Abdelilah, S., Rangini, Z., Belak, J., and Boggs, C. (1996). A genetic screen for mutations affecting embryogenesis in zebrafish. *Development* **123,** 37–46.

Grodzinski, Z. (1925). Beiträge zur Entwicklung der Blutgefäβe der Salmonidenembryonem. *Bull. Acad. Pol.* **Bd 2,** 623–631.

Grodzinski, Z., and Hoyer, H. (1938). Das Blutgefäβsystem. *In* "Klassen und Ordnungen des Tierreichs, Echte. Fische" (H. G. Bronns, Ed.), Vol. Bnd. 6, Teil 2, pp. 1–77, Akademiscaer Verlagsgeselleschaft m. b. H., Leipzig.

Haffter, P., Granato, M., Brand, M., Mullins, M. C., Hammerschmidt, M., Kane, D. A., Odenthal, J., van Eeden, F. J., Jiang, Y. J., Heisenberg, C. P., Kelsh, R. N., Furutani-Seiki, M., Vogelsang, E., Beuchle, D., Schach, U., Fabian, C., and Nusslein-Volhard, C. (1996). The identification of genes with unique and essential functions in the development of the zebrafish, *Danio rerio*. *Development* **123,** 1–36.

Isida, Z. (1956). Disvolvigo de kalateralaj vejnoj sur la ovoflavsako de kokojo. *Kaibogaku Zasshi* **31,** 334–348. [in Japanese, Esperanto summary]

Isogai, S., and Horiguchi, M. (1997). The earliest stages in the development of the circulatory system of the rainbow trout *Oncorhynchus mykiss*. *J. Morphol.* **233,** 215–236.

Iuchi, I., and Yamamoto, M. (1983). Erythropoiesis in the developing rainbow trout, *Salmo gairdneri irideus*: Histochemical and immunocemical detection of erythropoietic organs. *J. Exp. Zool.* **226,** 409–417.

Kawanishi, H. (1956). Disvolvigo de sangvazoj de ovoflavsako ce testudoj. *Caretta olivacea*. *Kaibogaku Zasshi* **31,** 517–550. [in Japanese, Esperanto summary.

Copyright © 2001 by Academic Press. All rights of reproduction in any form reserved.

Kilarski, W. (1958). The development of the blood vessels in the folds of the intestine of the seatrout (*Salmo trutta* L). *Acta Biol. Cracov.* **1,** 69–82.

Kimmel, C. B., Ballard, W. W., Kimmel, S. R., Ullmann, B., and Schilling, T. F. (1995). Stages of embryonic development in the zebrafish. *Dev. Dyn.* **203,** 253–310.

Olko, A. (1955). The respiratory vessels of the yolk-sac of the trout *Salmo trutta* L. *Zool. Pol.* **6,** 216–225.

Reagan, F. P. (1915). Vascularization phenomena in fragments of embryonic bodies completely isolated from yolk-sac blastoderm. *Anat. Rec.* **9,** 329–341.

Rieb, J.-P. (1973). La circulation sanguine chez l'embryon de *Brachydanio rerio. Ann. Embryol. Morphog.* **6,** 43–54.

Sabin, F. R. (1917). Origin and development of the primitive vessels of the chick and of the pig. *Contrib. Embryol.* **6,** 61–124.

Saito, H. (1984). The development of the spleen in the Australian Lungfish *Neoceratodus forsteri* Krefft, with special reference to its relationship to the "gastro"-enteric vasculature. *Am. J. Anat.* **169,** 337–360.

Stainier, D. Y., Weinstein, B. M., Detrich, H. W., 3rd, Zon, L. I., and Fishman, M. C. (1995). *Cloche*, an early acting zebrafish gene, is required by both the endothelial and hematopoietic lineages. *Development* **121,** 3141–3150.

Stainier, D.Y.R., Fouquet, B., Chen, J.-N., Warren, K. S., Weinstein, B. M., Meiler, S., Mohideen, M.-A. P. K., Neuhauss, S. C. F., Solnica-Krezel, L., Schier, A. F., Zwartkruis, F., Stemple, D. L., Malicki, J., Driever, W., and Fishman, M. C. (1996). Mutations affecting the formation and function of the cardiovascular system in the zebrafish embryo. *Development* **123,** 285–292.

Strawinski, M. S. (1949). The development of the liver vessels of the sea-trout L *Salmo trutta* L. *Bull. Acad. Sci. Cracov.* **2,** 435–446.

Swaen, A., and Brachet, A. (1899). Etude sur les premières phases du dıveloppement des organes dérivés du mésoblaste chez les poissons téléostéens. *Arch. Biol.* **16,** 173–311.

Tada, Y. (1956). Disvolvigo de sangvazoj sur la ovoflavsako kaj ankau de la mesintesto ce hamsteroj (*Cricetus anuratus*). *Kaibogaku Zasshi* **31,** 388–417. [in Japanese, Esperanto summary]

Ura, R. (1949). The study on the vascular system of the amphioxus. *Okayama Daigaku Igakubu. Kiyo.* **1,** 96–124. [in Japanese]

Ura, R. (1956). Pri la unuaj vojoj de sangvazoj kaj ilia sorto ce rajoj, trygon stephen. *Okajimas. Folia. Anat. Jpn.* **28,** 413–419. [in Esperanto]

Vernier, J.-M. (1969). Table chronologique du développement embryonnaire de la truite arc-en-ciel *Salmo gairdneri* Rich 1863. *Ann. Embryol. Morphol.* **2,** 495–520.

Weinstein, B. M., Stemple, D. L., Driever, W. D., and Fishman, M. C. (1995). *Gridlock*, a localized heritable vascular patterning defect in the zebrafish. *Nat. Med.* **11,** 1143–1147.

Westerfield, M. (1995). "The zebrafish book." Univ. of Oregon Press, Eugene, OR.

Yamada, H. (1951). The blood vascular system of the post-branchial alimentary canal in the lamprey. *Okayama Igakkai Zasshi* **63,** 1–51. [in Japanese]

Zhong, T. P., Rosenberg, M., Mohideen, M.-A. P. K., Weinstein, B., and Fishman, M. C. (2000). *Gridlock*, an HLH Gene for Assembly of the Aorta in Zebrafish. *Science* **287,** 1820–1824.

Received August 28, 2000
Accepted October 26, 2000
Published online January 10, 2001

Copyright © 2001 by Academic Press. All rights of reproduction in any form reserved.